The Journal of Immunology

Differential Regulation of $P2X_7$ Receptor Activation by Extracellular Nicotinamide Adenine Dinucleotide and Ecto-ADP-Ribosyltransferases in Murine Macrophages and T Cells

Shiyuan Hong, Nicole Schwarz, Anette Brass, Michel Seman, Friedrich Haag, Friedrich Koch-Nolte, William P. Schilling and George R. Dubyak

J Immunol 2009; 183:578-592; ;
doi: 10.4049/jimmunol.0900120
http://www.jimmunol.org/content/183/1/578

The Journal of Immunology is published twice each month by
The American Association of Immunologists, Inc.,
1451 Rockville Pike, Suite 650, Rockville, MD 20852

Print ISSN: 0022-1767 Online ISSN: 1550-6606.

Differential Regulation of $P2X_7$ Receptor Activation by Extracellular Nicotinamide Adenine Dinucleotide and Ecto-ADP-Ribosyltransferases in Murine Macrophages and T Cells

Shiyuan Hong,* Nicole Schwarz,† Anette Brass,† Michel Seman,‡ Friedrich Haag,† Friedrich Koch-Nolte,† William P. Schilling,* and George R. Dubyak[1]*

Extracellular NAD induces the ATP-independent activation of the ionotropic $P2X_7$ purinergic receptor ($P2X_7R$) in murine T lymphocytes via a novel covalent pathway involving ADP-ribosylation of arginine residues on the $P2X_7R$ ectodomain. This modification is catalyzed by ART2.2, a GPI-anchored ADP-ribosyltransferase (ART) that is constitutively expressed in murine T cells. We previously reported that ART2.1, a related ecto-ART, is up-regulated in inflammatory murine macrophages that constitutively express $P2X_7R$. Thus, we tested the hypothesis that extracellular NAD acts via ART2.1 to regulate $P2X_7R$ function in murine macrophages. Coexpression of the cloned murine $P2X_7R$ with ART2.1 or ART2.2 in HEK293 cells verified that $P2X_7R$ is an equivalent substrate for ADP-ribosylation by either ART2.1 or ART2.2. However, in contrast with T cells, the stimulation of macrophages or HEK293 cells with NAD alone did not activate the $P2X_7R$. Rather, NAD potentiated ATP-dependent $P2X_7R$ activation as indicated by a left shift in the ATP dose-response relationship. Thus, extracellular NAD regulates the $P2X_7R$ in both macrophages and T cells but via distinct mechanisms. Although ADP-ribosylation is sufficient to gate a $P2X_7R$ channel opening in T cells, this $P2X_7R$ modification in macrophages does not gate the channel but decreases the threshold for gating in response to ATP binding. These findings indicate that extracellular NAD and ATP can act synergistically to regulate $P2X_7R$ signaling in murine macrophages and also suggest that the cellular context in which $P2X_7R$ signaling occurs differs between myeloid and lymphoid leukocytes. *The Journal of Immunology,* **2009, 183: 578–592.**

The $P2X_7$ purinergic receptor ($P2X_7R$)[2] is an ATP-gated, nonselective cation channel that is predominantly expressed in cells of hematopoietic origin, including macrophages and T lymphocytes (1). The subunit structure of this 595-aa receptor includes two transmembrane segments, an intracellular N terminus, an intracellular C terminus, and a large extracellular loop (47–329 aa) that contain a presumed site or sites for ATP binding (2). Three of these $P2X_7$ subunits assemble to form the trimeric $P2X_7R$ channel (3). Stimulation of the $P2X_7R$ with extracellular ATP rapidly triggers increased Na^+, K^+, and Ca^{2+} fluxes across the plasma membrane (2), followed by the delayed induction of a nonselective pore that facilitates the permeation of molecules up to 900 Da in mass (4). Given its expression in myeloid and lymphoid leukocytes, many studies have identified roles for the $P2X_7R$ in the regulation of various proinflammatory and immune responses (reviewed in Refs. 5–7).

An unusual and defining feature of the $P2X_7R$ is its high threshold for activation by extracellular ATP ($EC_{50} \sim 500\ \mu M$); this contrasts with much lower activation thresholds for the other six members of the P2X family ($EC_{50} \sim 10\ \mu M$) (1, 8, 9). Intracellular ATP concentration is only 3–5 mM, and most cells express significant ecto-ATPase activities. Thus, it is unlikely that submillimolar levels of extracellular ATP can be sustained for significant durations within interstitial tissue compartments except perhaps during a massive lysis of host cells or the killing of invading pathogens. Clearly, the $P2X_7R$ is activated within in situ inflammatory loci or during normal development as indicated by the reduced levels of cytokines that accumulate within the inflamed footpads of $P2X_7R$ knockout mice (10), as well as the marked changes in bone density during the aging of these mice (11). Autocrine activation of $P2X_7R$ via the release of endogenous ATP has been recently reported in human monocytes in response to LPS stimulation of TLR4 signaling (12, 13) and in T cells in response to Ag stimulation of TCR signaling cascades (14). This released ATP may accumulate within diffusion-restricted microdomains of the cell surface, such as caveolar or nascent endosomal invaginations not readily accessible to the bulk extracellular medium.

However, physiological $P2X_7R$ activation may involve modes of regulation in addition to autocrine stimulation. One of these modes is allosteric modulation of ATP affinity via conformational changes in $P2X_7$ trimeric channels produced by local biophysical conditions such as pH, ionic composition (15–17), or membrane lipid composition (18). For example, lysophosphatidylcholine and other lysolipids reduce the threshold level of ATP required for

*Department of Physiology and Biophysics, Case Western Reserve University School of Medicine, Cleveland, OH 44120; †Institute of Immunology, University Hospital, Hamburg, Germany; and ‡University of Rouen, Rouen, France

Received for publication January 14, 2009. Accepted for publication May 5, 2009.

The costs of publication of this article were defrayed in part by the payment of page charges. This article must therefore be hereby marked *advertisement* in accordance with 18 U.S.C. Section 1734 solely to indicate this fact.

[1] Address correspondence and reprint requests to Dr. George R. Dubyak, Department of Physiology and Biophysics, Case Western Reserve University School of Medicine, 10900 Euclid Avenue, Cleveland OH, 44120. E-mail address: george.dubyak@case.edu

[2] Abbreviations used in this paper: $P2X_7R$, $P2X_7$ receptor; ADP-R, ADP-ribose; ART, ADP-ribosyltransferase; BMDM, bone marrow-derived macrophage; BSS, basic salt solution; εNAD, etheno-NAD; GSH, glutathione; iNOS, inducible NO synthase; $mP2X_7$, murine $P2X_7$; NZW, New Zealand White; PS, phosphatidylserine; WT, wild type.

www.jimmunol.org/cgi/doi/10.4049/jimmunol.0900120

$P2X_7R$-dependent Ca^{2+} influx and pore formation in murine microglia (19). Another type of regulation involves the gating of $P2X_7R$ channels by mechanisms independent of reversible ATP binding. Notably, extracellular NAD induces the ATP-independent activation of $P2X_7R$ in murine T lymphocytes via a novel covalent pathway involving ADP-ribosylation of arginine residues on the $P2X_7R$ ectodomain (20–22).

The ADP-ribosylation of $P2X_7R$ is catalyzed by ART2, a GPI-anchored ADP-ribosyltransferase (ART) constitutively expressed on the cell surface of murine T cells (23–25). ART2 belongs to a family of ectoenzymes that use extracellular NAD to transfer the ADP-ribose (ADP-R) moiety to substrate proteins (26). ART2 mediates $P2X_7R$ transactivation via ADP-ribosylation of the R125 residue within the extracellular loop of the receptor (21). This covalent modification apparently mimics the conformational changes in $P2X_7R$ induced by noncovalent ATP binding and triggers both Ca^{2+} influx and the secondary nonselective pore permeable to fluorescent dyes. The NAD- and ART2-dependent activation of $P2X_7R$ consequently induces phosphatidylserine (PS) exposure on T cell surfaces, increased shedding of CD62L, and acceleration of T cell death. Other studies have shown that extracellular NAD induces $P2X_7R$ activation in in vivo models of immune and inflammatory responses (21, 27, 28).

ART2 includes two isoforms, ART2.1 and ART2.2, which are encoded by tandem genes (*Art2a* and *Art2b*) located on murine chromosome 7 (26). Although ART2.1 is functionally and structurally similar to ART2.2, it contains two additional cysteine residues (Cys^{80} and Cys^{201}) that readily form a disulfide bond that allosterically suppresses catalytic activity (29). This inhibited state of ART2.1 is reversed by extracellular thiol reductants, such as exogenous DTT or the endogenous cysteine and glutathione released by inflamed or damaged tissues (30, 31). T cells from most inbred mouse strains (e.g., BALB/c) natively express both ART2.1 and ART2.2 (25, 32–34). However, the latter isoform is sufficient for NAD-induced $P2X_7R$ activation and cell death, because these responses occur in the absence of extracellular thiol reductants and in T cells from C57BL/6 mice that express a mutated *Art2a* gene and no functional ART2.1 protein (20, 35).

Although the NAD-induced, ART2-dependent mechanism is clearly a major pathway for $P2X_7R$ activation in mouse T lymphocytes, it is unclear whether this mechanism is operative in macrophages, another class of leukocytes that natively express $P2X_7R$ at high levels. Relevant to this issue, we have reported the inducible expression of ART2.1, but not ART2.2, in murine bone marrow-derived macrophages (BMDM) stimulated by multiple inflammatory factors (36). This prompted us to examine the role of ART2.1 as a regulator of $P2X_7$ receptors natively expressed in murine macrophages or heterologously expressed in HEK293 cells. We demonstrate that coexpression of the murine $P2X_7R$ with ART2.1 or ART2.2 in HEK293 cells facilitates similar NAD-driven ADP-ribosylation of the receptor. However, NAD stimulation of $P2X_7R$ in macrophages or HEK293 cells is not sufficient to activate the receptor. Rather, the NAD/ART2-dependent modification of the $P2X_7R$ potentiates the ability of ATP to activate the receptor as indicated by a left shift in the ATP dose-response relationship. Thus, extracellular NAD acts to regulate the ionotropic $P2X_7R$ in both macrophages and T cells but via distinct mechanisms on the gating of channel activity. These observations support a role for extracellular NAD in the regulation of $P2X_7R$-dependent inflammatory responses in macrophages and additionally suggest that the cellular context (i.e., myeloid vs lymphoid cells) dictates the outcome of signaling through the $P2X_7R$.

Materials and Methods

Materials

Recombinant murine IFN-γ was from Boehringer Mannheim Biochemica and recombinant murine IFN-β was from US Biologicals. LPS (*Escherichia coli* serotype 01101:B4) was from List Biological Laboratories. ATP, NAD, etheno-NAD (εNAD), ADP-R, reduced glutathione (GSH), and TRIzol were from Sigma-Aldrich. Oligo(dT) primer was from Promega. Avian myeloblastosis virus reverse transcriptase was from Roche. Tag DNA polymerase was from New England Biolabs. The 1G4 mouse mAb (a generous gift from Dr. R. Santella, Columbia University, New York, NY) was prepared as previously described (36). Fura-2-AM, ethidium bromide, allophycocyanin-conjugated annexin V and YO-PRO-1 were from Molecular Probes. The anti-$P2X_7R$ K1G Ab and mAbs directed against mouse ART2.1 or ART2.2 were generated and used as recently described (37). BALB/c, C57BL/6, and New Zealand White (NZW) mice were purchased from Taconic Farms. $P2X_7R^{-/-}$ mice were originally provided by Pfizer Global Research and Development and then backcrossed into a pure C57BL/6 background for >12 generations from a $P2X_7R^{-/-}$ mouse strain described previously (38). All experiments and procedures involving mice were approved by the Institutional Animal Use and Care Committees of Case Western Reserve University (Cleveland, OH) or Hamburg University Hospital (Hamburg, Germany).

Cell culture and animals

BMDM and splenocytes isolated from BALB/c, C57BL/6, NZW, or $P2X_7R^{-/-}$ mice were prepared as previously described (36). Bac1.2F5 murine macrophages were cultured in DMEM (Sigma-Aldrich) supplemented with 25% L cell-conditioned medium, 15% calf serum (HyClone Laboratories), 100 U/ml penicillin, and 100 μg/ml streptomycin (Invitrogen) in the presence of 10% CO_2. RAW264.7 macrophages were cultured in DMEM supplemented with 10% calf serum, 100 U/ml penicillin, and 100 μg/ml streptomycin in the presence of 10% CO_2. Where indicated, BMDM or the macrophage cell lines (Bac1.2F5 and RAW264.7) were primed for 24 h with either LPS (100 ng/ml), IFN-γ, (100 U/ml), or IFN-β (100 U/ml) to induce an inflammatory phenotype and the up-regulation of ART2.1 expression. Murine BW5147 T lymphoma cells were maintained in RPMI 1640 supplemented with 10% calf serum and 1% penicillin-streptomycin in the presence of 5% CO_2. Wild-type (WT) HEK293 cells were cultured in DMEM supplemented with 10% calf serum and 1% penicillin-streptomycin in the presence of 10% CO_2. HEK293 cells stably transfected with either the WT murine $P2X_7R$ (HEK-m$P2X_7$ cells) or the mutant R276K $P2X_7R$ (HEK-m$P2X_7$-R276K cells) were selected and maintained in DMEM supplemented with 400 μg/ml G418 or 10 μg/ml blasticidin. The ART2 plasmids were transiently transfected into HEK $P2X_7R$ cells using cells seeded at 6×10^5 per 35-mm dish 24 h before transient transfection. The cells were transfected using PolyFect reagent (Qiagen) with 2.5 μg of plasmid DNA per dish followed by incubation at 37°C for 36 h before experiments.

RT-PCR analyses

Total RNA was extracted using TRIzol; all primers and PCR conditions for ecto-ARTs, inducible NO synthase (iNOS), IFN-β, and GAPDH were prepared and used as previously described (36). The PCR amplicons were separated by 1.5% agarose gel electrophoresis and visualized by ethidium bromide staining; the resulting fluorescence images were recorded with a BioRad Gel Doc 1000 system.

1G4 mAb-based assay of ART2 activity

ART activity in intact Bac1.2F5 macrophages, RAW264.7 macrophages, or BW5147 T lymphocytes was assayed using a Western blot protocol based on the 1G4 mAb as previously described (36). Briefly, intact cells were transferred to basic salt solution (BSS) containing 130 mM NaCl, 5 mM KCl, 1.5 mM $CaCl_2$, 1 mM $MgCl_2$, 25 mM HEPES (pH 7.5), 5 mM glucose, and 0.1% BSA. The cells were incubated at 37°C for 15 min with 50 μM ε-NAD and 1 mM ADP-R in the presence of 1 mM DTT before extraction, SDS-PAGE, and Western blotting.

Labeling and immunoprecipitation of ADP-ribosylated $P2X_7R$

HEK293 cells were harvested by trypsinization at 20 h after cotransfection with $P2X_7R$ and either ART2.1 or ART2.2. ART2/$P2X_7R$-coexpressing HEK cells were then incubated at 37°C for 15 min with 50 μM ^{32}P-NAD and 1 mM ADP-R in the presence or absence of 1 mM DTT. Washed cells were lysed in PBS, 1% Triton-X100, 1 mM 4-(2-aminoethyl)-benzenesulfonyl fluoride (Sigma-Aldrich) for 20 min at 4°C. Insoluble material was pelleted by high-speed centrifugation (for 15 min at 13,000 $\times$ *g*). K1G Ab

at 3 μg/ml (39) was added into the lysate and incubated for 2 h at 4°C, and lysates were further incubated with protein G-Sepharose beads (20 μl beads/lysates from 10^6 cells) for 60 min at 4°C. Immunoprecipitates were washed three times using Triton X-100 buffer. The final product was eluted into 30 μl of 2× SDS binding buffer and boiled for 5 min. The samples were loaded onto 15% SDS-polyacrylamide gels and proteins were detected by autoradiography. P2X$_7$ was detected with a rabbit anti-P2X$_7$ C-terminal peptide Ab (1/1000) (Alomone Labs) and peroxidase-conjugated anti-rabbit IgG (1/5000) using the ECL system (Amersham-GE Healthcare).

FACS analysis

Staining for the P2X$_7$R was performed with Alexa Fluor 488-conjugated K1G Ab for 30 min at 4°C (39). Stained cells were washed and analyzed on a FACSCalibur flow cytometer using CellQuest software (BD Biosciences). Gating was performed on living cells on the basis of propidium iodide exclusion.

Measurement of P2X$_7$R-mediated Ca^{2+} influx or nucleotide-induced Ca^{2+} mobilization

Macrophages (primary BMDM or macrophage cell lines) were collected in DMEM by gently scraping the monolayers and transferring the detached cells into 50-ml tubes. HEK293 cells were detached by trypsinization. The detached macrophages or HEK293 cells were centrifuged and the cell pellets were washed twice with BSS. Primary spleen lymphocytes or BW5147 T cell suspensions were directly pelleted from growth medium before washing. Washed cells were resuspended in BSS supplemented with 1 μM fura-2-AM and incubated at 37°C for 40 min. The fura-2-loaded cells were then washed, resuspended in BSS (10^6/ml), and then stored on ice for up to 3 h during measurements. For each measurement, a 1.5-ml aliquot of cell suspension was stirred at 37°C in a quartz cuvette for measurement of fura-2-AM fluorescence (339 nm excitation/500 nm emission) and calibration as previously described (40). Murine macrophages (41, 42) and HEK293 cells (43, 44) also express several subtypes of G protein-coupled, Ca^{2+}-mobilizing P2Y receptors. Thus, the macrophages or HEK293 cells were first treated with a mixture of 50 μM ADP and 50 μM UTP to activate and desensitize these P2Y receptors before P2X$_7$R stimulation by the indicated concentrations of ATP or NAD (45). In some experiments, P2Y receptor-dependent Ca^{2+} mobilization in Bac1.2F5 macrophages or BW5147 T lymphocytes was directly assayed by stimulating the cells with 30 μM ADP, UTP, or UDP. Where indicated, the macrophages or HEK293 cells were treated in the presence or absence of 1 mM DTT (plus 1 mM ADP-R) for 1–5 min before stimulation with 10–100 μM NAD.

Measurement of P2X$_7$R-mediated YO-PRO-1 or ethidium dye uptake

HEK293 cells transfected with ART2.1 and the hyperresponsive R276K P2X$_7$R variant (21) were gently trypsinized and incubated in the absence or presence of NAD or ATP in 10 mM HEPES (pH 7.5), 140 mM NaCl, 5 mM KCl, 10 mM glucose, and 1 μM YO-PRO-1 (Molecular Probes) for 60 min at 37°C. Cells were subsequently washed, resuspended in annexin V binding buffer (BD Biosciences), and stained with annexin V-allophycocyanin (BD Biosciences) before analysis by flow cytometry. Spleen cells from BALB/c or NZW mice were incubated with YO-PRO-1 as described above, stained with Abs against the surface markers CD3 and B220, and analyzed by flow cytometry. Cells staining positive for CD3 were analyzed for the expression of P2X$_7$R, ART2.1, ART2.2, and the uptake of YO-PRO-1. Control or IFN-γ-primed Bac1.2F5 macrophages were collected in DMEM by gently scraping of the monolayers and transfer into 50-ml tubes. The cells were centrifuged, washed, and resuspended in BSS. Aliquots (1.5 ml) of cell suspension were transferred to the stirred measuring cuvette and preincubated for 3 min at 37°C. Ethidium bromide (2.5 μM) was added and baseline fluorescence (360 nm excitation/580 nm emission) was recorded before stimulation of the cells with various concentrations of NAD and/or ATP as described in the Fig. 10 legend. All ethidium$^+$ fluorescence increases were corrected for background dye fluorescence. The P2X$_7$R-mediated increases in ethidium$^+$ accumulation were expressed as percentages of the maximal fluorescence observed when the cells were permeabilized with 0.003% digitonin.

HPLC analysis of extracellular NAD metabolism

Monolayers of Bac1.2F5 macrophages (10^6 cells/well in 6-well dishes) were incubated in 1 ml of BSS at 37°C supplemented with 100 μM NAD in the presence or absence of 1 mM ADP-R. At selected times (0–60 min), 100-μl aliquots of the extracellular medium were removed, boiled for 5 min, and centrifuged to sediment any precipitated protein. NAD and its principle metabolite, ADP-R, were separated and quantified using a reverse-phase HPLC protocol. Briefly, 50-μl aliquots were injected onto an Alltech C18 Adsorbosphere column that was isocratically eluted at 1.3 ml/min with a running buffer of 0.1 M KH_2PO_4 and 5% methanol (pH 6). NAD (elution time 8.2 min) and ADP-R (elution time 4 min) were detected by absorbance at 254 nm.

Statistics

All experiments were repeated 2–6 times using different preparations of primary leukocytes isolated from different mice or with leukocyte cell lines from separate cultures. All data, unless otherwise stated, represent mean ± SEM. A two-tailed, one-variable Student's *t* test was used to analyze these data with statistical significance defined as $p < 0.05$.

Results

NAD induces activation of P2X$_7$R in murine lymphocytes but not murine macrophages

We confirmed the ability of extracellular NAD to induce P2X$_7$R activation (as assayed by Ca^{2+} influx) in freshly isolated splenic lymphocytes from BALB/c or C57BL/6 mice (Fig. 1, *A* and *B*), but not in lymphocytes from P2X$_7^{-/-}$ mice (Fig. 1*C*). (Although splenic lymphocytes include both T cells and B cells, P2X$_7$R is not expressed by murine B cells; see Ref. 46). We tested lymphocytes from the BALB/c and C57BL/6 mouse strains because they express polymorphic variants of the P2X$_7$R (P451 for BALB/c and L451 for C57BL/6) (47). Additionally, T lymphocytes from BALB/c mice express both ART2.1 and ART2.2 as functional enzymes, whereas leukocytes from C57BL/6 mice express only ART2.2 due to a premature stop codon in ART2.1 mRNA that prevents translation of a functional protein (34, 35).

In contrast to its actions on T cells, NAD did not trigger Ca^{2+} influx in naive BMDM isolated from either BALB/c or C57BL/6 mice (Fig. 1, *D* and *E*) even though ATP stimulated robust increases in Ca^{2+} in both WT BMDM populations, but not in BMDMs from P2X$_7$R-deficient mice (Fig. 1*F*). This absence of an NAD effect in naive macrophages was consistent with our previous findings that murine macrophages express only low levels of ecto-ARTs in the absence of proinflammatory activation by IFNs or LPS. Likewise, C57BL/6 BMDM were unresponsive to NAD even after proinflammatory activation by LPS (Fig. 1*H*) or IFNs (not shown); this is consistent with the general lack of ART2.2 expression in murine myeloid leukocytes and the specific lack of ART2.1 expression in C57BL/6 myeloid leukocytes (35). As expected, neither NAD nor ATP elicited a Ca^{2+} influx response in P2X$_7$-knockout BMDM (Fig. 1*I*). Surprisingly, however, inflammatory BALB/c BMDM primed with IFN-γ (Fig. 1*G*) to up-regulate ART2.1 were also unresponsive to extracellular NAD but retained a robust response to ATP. We have previously described the use of anti-ART2.1, anti-ART2.2, and anti-εADP- mAbs in FACS analyses to confirm that LPS and IFN-γ induced the specific up-regulation of ART2.1 protein and ADP-ribosyltransferase activity in BMDM from WT BALB/c mice (36), but not in BMDM from an ART2.1 knockout BALB/c strain (data not shown). Consistent with the thiol dependence of ART2.1 enzyme activity, the inclusion of DTT markedly increases ADP-ribosylation of cell surface proteins in intact BALB/c BMDM (36). However, the inclusion of extracellular DTT did not facilitate NAD-induced Ca^{2+} influx in these IFN-primed BMDM (Fig. 1*G*).

The murine P2X$_7$R is a substrate for ADP-ribosylation and gating by the thiol-sensitive ART2.1 ectoenzyme

The ability of extracellular NAD to activate the P2X$_7$R in BALB/c T cells that express ART2.1 and ART2.2, but not in BALB/c macrophages that express only ART2.1, raised the critical question of whether ART2.1 (similarly as ART2.2) can recognize the P2X$_7$R as a substrate. To test this, the murine P2X$_7$R was coexpressed

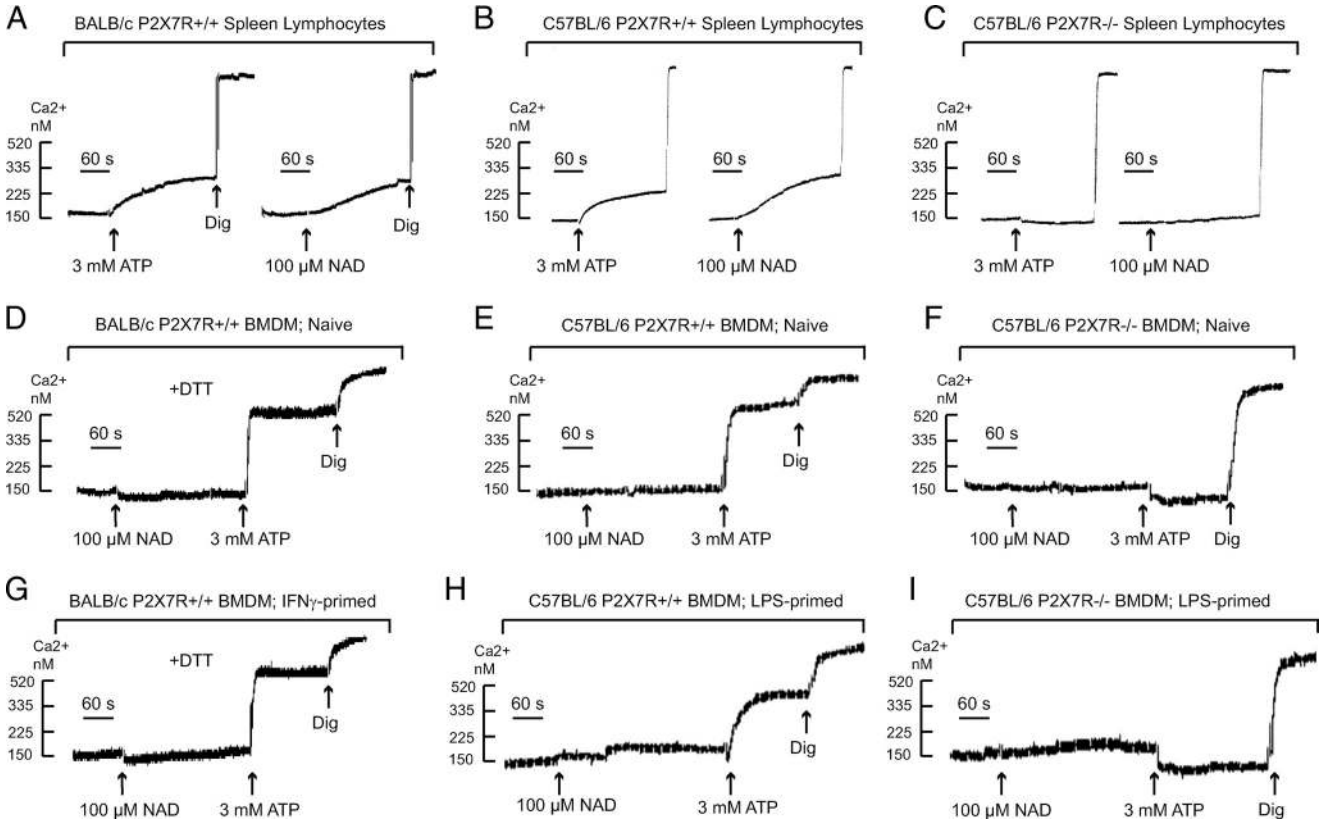

FIGURE 1. NAD induces the activation of $P2X_7R$ in murine lymphocytes but not murine macrophages. Changes in cytosolic Ca^{2+} in response to ATP (3 mM) or NAD (100 μM) were measured in fura-2-loaded suspensions of spleen lymphocytes or BMDM as described in *Materials and Methods*. Macrophage suspensions were pretreated with a mixture of 50 μM ADP and 50 μM UTP to activate and desensitize P2Y receptors 5 min before $P2X_7R$ stimulation by ATP or NAD. Where indicated, 1 mM DTT was included in the assay medium to support the activity of the thiol-sensitive ART2.1 ectoenzyme. All cells were permeabilized with digitonin (Dig) to release fura-2 for subsequent calibration. All traces are representative of observations from three to six experiments with the leukocyte preparations isolated from different mice of the noted strains. *A*, Freshly isolated spleen lymphocytes from BALB/c mice. *B*, Freshly isolated spleen lymphocytes from C57BL/6 mice. *C*, Freshly isolated spleen lymphocytes from the spleen of $P2X_7R$-knockout mice (C57BL/6 background). *D*, Naive BMDM from BALB/c mice. *E*, Naive BMDM from C57BL/6 mice. *F*, Naive BMDM from $P2X_7R$-knockout mice (C57BL/6 background). *G*, BMDM from BALB/c mice were primed with 100 U/ml IFN-γ for 24 h to induce ART2.1 expression before the Ca^{2+} assay. *H*, BMDM from C57BL/6 mice were primed with 100 ng/ml LPS plus 10 μM U0126 for 24 h to induce proinflammatory gene expression before the Ca^{2+} assay. *I*, BMDM from $P2X_7R$-knockout mice (C57BL/6 background) were primed with 100 ng/ml LPS plus 10 μM U0126 for 24 h to induce proinflammatory gene expression before the Ca^{2+} assay.

with ART2.1 or ART2.2 in HEK293 cells. The ART2-expressing cells were briefly incubated with [^{32}P]NAD in the presence or absence of DTT before extraction, immunoprecipitation of the $P2X_7R$, SDS-PAGE, and detection of [^{32}P]ADP-ribosylated $P2X_7R$ by autoradiography. Fig. 2*A* illustrates the extracellular domain of the $mP2X_7R$ including the relative positions of seven (of 18 total) arginine residues within this domain. Previous studies identified R125 and R133 as the critical sites for ART2.2-catalyzed ADP-ribosylation of the $P2X_7R$ (21). Thus, we compared WT $P2X_7R$ vs a $P2X_7R$ construct (R125K/R133K) wherein the two target arginines for ART2.2 within the cysteine-rich loop were replaced by lysine and, as a consequence, cannot function as an acceptor for ADP-ribosylation by ART2.2. The expression of ART2.1 in HEK293 cells facilitated the robust ADP-ribosylation of the WT $P2X_7R$, but not the double arginine mutant variant as assayed by incorporation of [^{32}P]ADP-R (Fig. 2*B*). Notably, the ability of ART2.1 to ADP-ribosylate the WT $P2X_7R$ was highly dependent on exogenously added DTT. In contrast, HEK293 cells coexpressing ART2.2 and WT $P2X_7R$ showed strong and equivalent [^{32}P]ADP-ribosylation of $P2X_7R$ in the absence or presence of DTT; mutants of $P2X_7$ in which the R125 and R133 residues were changed to lysine did not function as a substrate for ART2.2 regardless of the presence or absence of DTT (data not shown). Importantly, we used the K1G anti-$P2X_7$ Ab and FACS analyses to confirm similar cell surface expression levels of all WT and mutant $P2X_7R$ constructs (Fig. 2).

We next asked whether ADP-ribosylation of $P2X_7R$ by ART2.1 also induces the gating of $P2X_7R$. To this end, we examined NAD-induced and $P2X_7R$-dependent pore formation in T lymphocytes from BALB/c mice, which express both ART2.1 and ART2.2, or corresponding cells from NZW mice, which lack ART2.2 and express only ART2.1 (Fig. 2*C*). The formation of membrane pores that allow the incorporation of DNA-staining dyes like YO-PRO-1 is considered to be a typical hallmark of $P2X_7$ activation. Fig. 2*D* shows that T lymphocytes from BALB/c mice, which express high levels of ART2.2, incorporate YO-PRO-1 in response to micromolar NAD regardless of the presence or absence of DTT. In contrast, NAD-induced YO-PRO-1 uptake into T lymphocytes from NZW mice, which express only ART2.1, is strictly dependent on DTT and also requires higher concentrations of NAD.

NAD potentiates ATP-induced $P2X_7R$ activation in HEK293 cells coexpressing ART2 and $P2X_7R$

The data in Fig. 2 verified the ability of NAD to effectively ADP-ribosylate the WT murine $P2X_7R$ when heterologously expressed

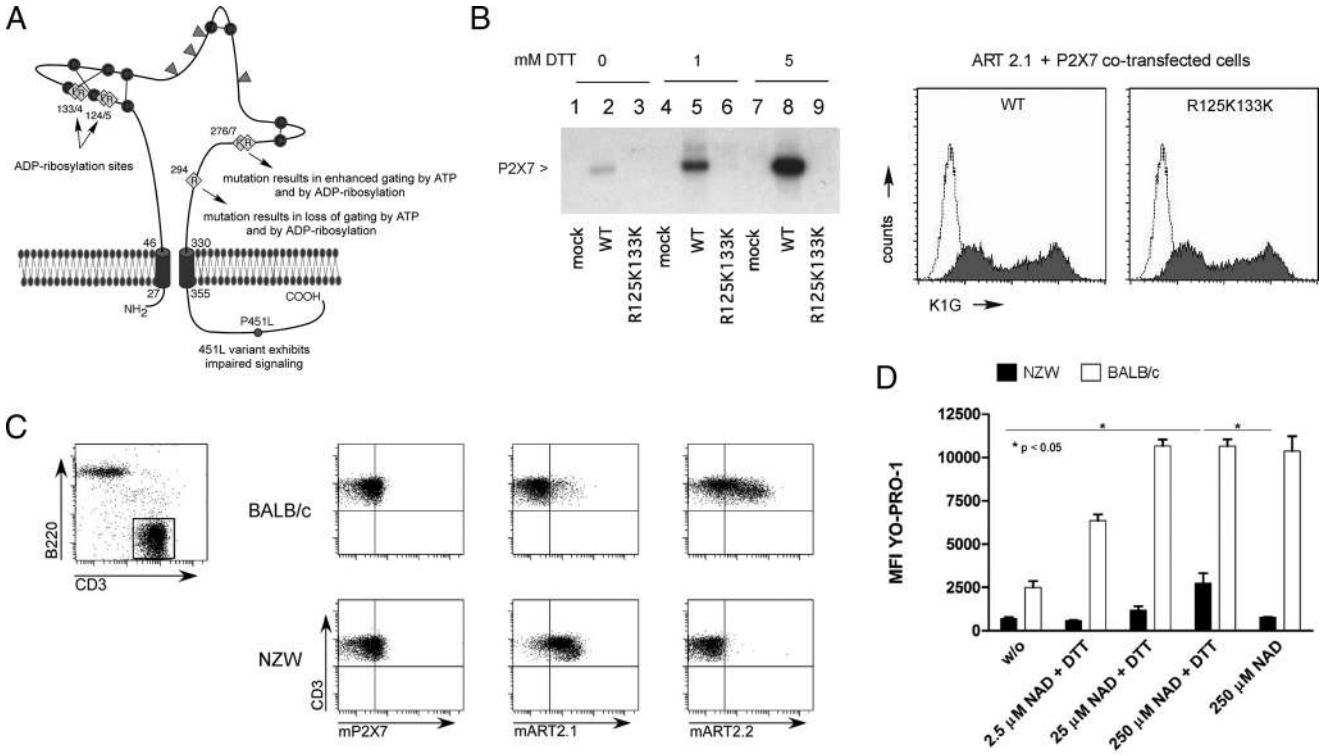

FIGURE 2. The murine P2X$_7$R is a substrate for ADP-ribosylation and gating by both the thiol-sensitive ART2.1 and the thiol-insensitive ART2.2. *A*, Schematic of murine P2X$_7$R showing the relative distribution of important arginine residues (diamonds), disulfide-bonded cysteine residues (circles), and *N*-linked glycosylation sites (arrowheads) in the extracellular ligand-binding domain, as well as the natural allelic 451L variant in the cytosolic domain of P2X$_7$R. *B*, HEK cells were cotransfected with WT murine P2X$_7$R plus murine ART2.1 or with an R125K/R133K double mutant of the murine P2X$_7$R (R125K133K) plus murine ART2.1. Aliquots of the control and transfected cells were stained with the anti-P2X$_7$ K1G Ab for FACS analysis as described in *Materials and Methods*. Parallel aliquots of the control (mock-tranfected) or cotransfected cells were incubated for 15 min with 50 μM [^{32}P]NAD and 1 mM ADP-R in the presence of the indicated concentrations of DTT before lysis and immunoprecipitation with the K1G Ab; immunoprecipitated products were resolved by SDS-PAGE and detected by autography. Results are representative of observations from two or more independent experiments. *C*, FACS analysis of splenocytes from BALB/c and NZW mice. CD3-expressing T lymphocytes (*left panel*) were analyzed for surface expression of P2X$_7$R, ART2.1, and ART2.2 (*right panels*). *D*, Splenocytes were incubated with the fluorescent dye YO-PRO-1 and NAD and DTT as indicated. The mean fluorescence intensity (MFI) in the YO-PRO-1 channel of cells gated for CD3 expression as in *C* was measured as an indication of pore formation in T lymphocytes. Data bars show the mean $\pm$ SE of the MFI values from three independent experiments for each T cell type with $p < 0.05$ for the indicated comparisons in the NZW data sets.

with ART2.1 in the HEK293 cell background. However, we have reported that this covalent modification of the WT P2X$_7$R expressed in HEK293 cells is not sufficient for functional activation of the receptor (21). Fig. 3*A* shows this by comparing NAD with ATP as stimuli for Ca^{2+} influx in a HEK293 line (HEK-mP2X$_7$ cells) stably transfected with murine P2X$_7$R cDNA before transient transfection with an ART2.2 expression plasmid. Western blot analysis confirmed the expression of functional ART activity in ART2.2-transfected, but not parental, HEK293 cells (Fig. 3*C*). This assay involves incubation of intact cells with εNAD (an NAD analog) to covalently ε-ADP-ribosylate cell surface proteins followed by cell extraction, SDS-PAGE, and probing with the anti-ε-ADP-R 1G4 mAb. Fig. 3*C* also shows that inclusion of extracellular ADP-R potentiated the accumulation of ADP-ribosylated proteins by attenuating the metabolism of εNAD (or NAD) by ectonucleotidases. Despite the robust ART activity in the cotransfected HEK-mP2X$_7$ cells, extracellular NAD did not mimic the ability of ATP to trigger P2X$_7$R-dependent Ca^{2+} influx.

We have described another P2X$_7$R arginine residue (R276) that is not an ecto-ADP-ribosylation site but is a critical modulator of ATP potency (21). Fig. 3*B* shows that the HEK293 line (HEK-mP2X$_7$-R276K), stably transfected with the R276K gain of function mutant of P2X$_7$R, exhibited a maximal Ca^{2+} influx response to 50 μM ATP, which is a subthreshold concentration in cells expressing WT P2X$_7$R (see Fig. 4*A*). Notably, this R276K mutation also facilitated the gating of P2X$_7$R channel activity in response to NAD in HEK293 cells cotransfected with ART2.2 (Fig. 3*B*).

Fig. 3*D* demonstrates that ART2.1 also mediates the NAD-dependent activation of the hypersensitive R276K mutant P2X$_7$R in transiently cotransfected HEK293 cells. These experiments used two FACS-based readouts of P2X$_7$R function: 1) the transfer of PS to the external leaflet of the plasma membrane bilayer ("PS-flip") as measured by increased binding of fluorochrome-conjugated annexin V; and 2) induction of the nonselective permeability pore as measured by the influx of YO-PRO-1 dye. In the absence of either ATP or NAD stimuli, the cells exhibited little if any surface annexin V staining or YO-PRO-1 accumulation. When stimulated by ATP, the majority of the ART2.1-mP2X$_7$-R276K-cotransfected HEK cells showed strongly increased annexin V binding and YO-PRO-1 uptake. Treatment with NAD in the presence of DTT caused a similar stimulation of annexin V binding but a somewhat lower induction of YO-PRO-1 uptake. In contrast, cells treated with ADP-R plus DTT exhibited control levels of annexin binding and dye accumulation. Notably, these PS-flip and YO-PRO-1 influx responses to NAD were absent when the R276K mutation was combined with the double R125K/R133K substitutions that

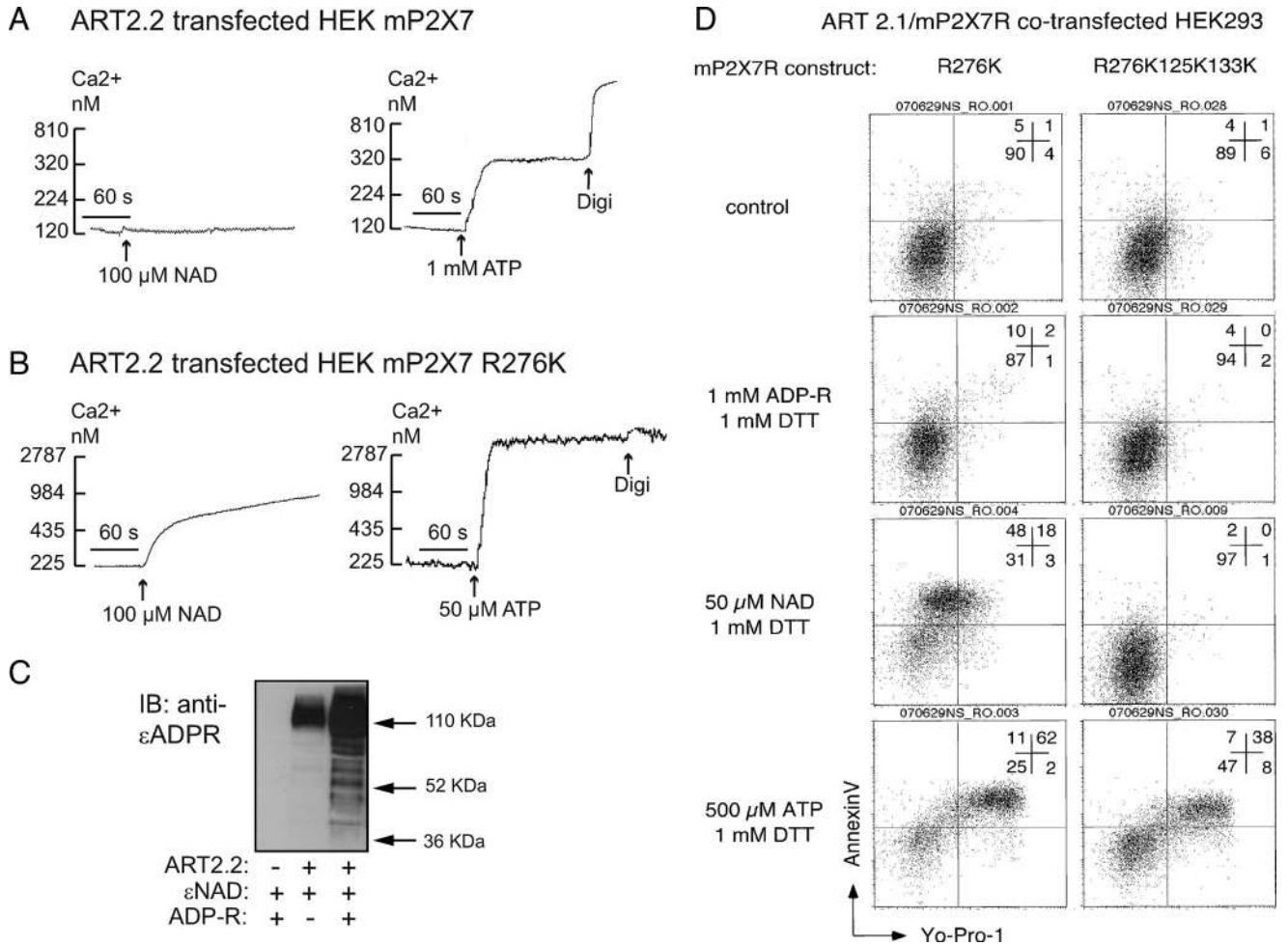

FIGURE 3. Differential effects of NAD/ART2 on activation of the murine $P2X_7R$ vs R276K-mutated $P2X_7R$ in HEK293 cells. *A* and *B*, HEK293 cells were stably transfected with either WT murine $P2X_7R$ (HEK-m$P2X_7$ cells) in *A* or the R276K mutant of murine $P2X_7R$ (HEK-m$P2X_7$-R276K cells) in *B*. The stably transfected lines were transiently cotransfected with murine ART2.2 24 h before an analysis of $P2X_7R$-dependent Ca^{2+} influx was conducted. Cytosolic Ca^{2+} was measured in fura-2-loaded HEK cell suspensions as described in *Materials and Methods* and Fig. 1. The cell suspensions were pretreated with a mixture of 50 μM ADP and 50 μM UTP to activate and desensitize P2Y receptors 5 min before $P2X_7R$ stimulation by the indicated concentrations of ATP or NAD. NAD was added together with 1 mM ADP-R to attenuate metabolism of the NAD. These traces are representative of observations from three to four experiments with each cell line. Digi, Digitonin. *C*, HEK293 cells were transiently mock transfected (*left lane*) or transfected with ART2.2 (*middle* and *right lanes*). After 36 h, the intact cells were acutely incubated for 15 min with 50 μM ε-NAD with or without 1 mM ADP-R before extraction, SDS-PAGE, and Western blotting with the 1G4 mAb that detects ε-ADP-ribosylated proteins. IB, Immunoblotting. *D*, HEK cells were transiently cotransfected with murine ART2.1 and the indicated murine $P2X_7R$ mutants (R276K single mutant or R125K/R133K/R276K (R276K125K133K) triple mutant) before experiments. At 20 h posttransfection, the cells were harvested by trypsinization without further treatment (control) or following 10-min incubations with 1 mM ADP-R, 50 μM NAD, or 500 μM ATP separately in the presence of 1 mM DTT. The cells were then treated with 1 μM YO-PRO-1 for 1 h. Aliquots of the cotransfected cells were stained with allophycocyanin-conjugated annexin V before FACS analysis. All results are representative of observations from two or more independent experiments. The numbers in each panel represent the percentages of cells in the respective quadrants.

eliminate the $P2X_7$ ADP-ribosylation sites targeted by ART2.1. In contrast, and in accord with our previous report (21), the triple R276K/R125K/R133K mutant of $P2X_7$ retained robust responses to ATP.

The differential ability of NAD/ART2 to activate the R276K-mutated $P2X_7R$ (Fig. 3, *B* and *D*), but not the WT $P2X_7R$ (Fig. 3*A*), in an HEK293 background is similar to the observations in Fig. 1 regarding the differential ability of NAD to activate $P2X_7R$ in murine T lymphocytes, but not in murine macrophages. These differences indicate that the consequences of ADP-ribosylation on $P2X_7R$ function are cell type specific, perhaps due to the differential expression of cell-specific accessory signaling molecules or of variant forms of $P2X_7R$. We tested the hypothesis that ADP-ribosylation of WT $P2X_7R$ in HEK293 cells, although insufficient to activate the receptor per se, might modulate the ATP activation threshold. HEK293 cells coexpressing ART2.2 and WT $P2X_7R$ were prestimulated with or without 100 μM NAD for 3–5 min before being challenged with increasing concentrations of ATP to activate $P2X_7R$-mediated Ca^{2+} influx. The NAD pretreatment decreased the threshold concentration of ATP required to stimulate $P2X_7R$ in cells that coexpressed ART2 (Fig. 4, *A* and *B*). In Fig. 4, *C–F* compare the quantification of ATP-induced changes in Ca^{2+} (with or without NAD pretreatment) at 30 s (Fig. 4, *C* and *E*) and 3 min (Fig. 4, *D* and *F*) in ART2-transfected or -nontransfected HEK-m$P2X_7$ cells. The NAD-induced shift in ATP sensitivity was most apparent with [ATP] in the 200–600 μM range. NAD did not further increase the Ca^{2+} influx response to [ATP] $\geq$ 1 mM, which maximally activates $P2X_7R$ function. Notably, NAD pretreatment did not shift the ATP dose-response relationship in

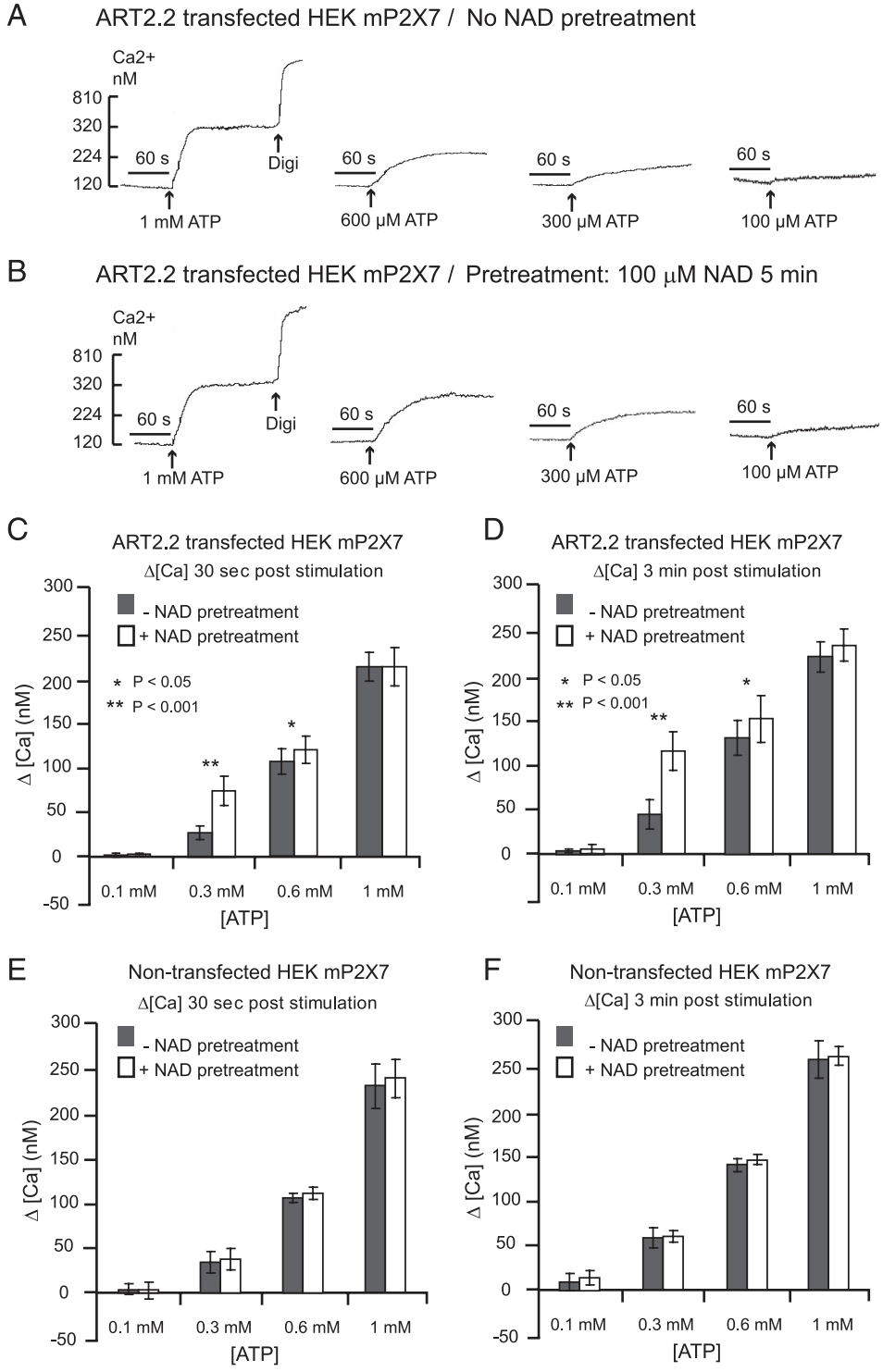

FIGURE 4. NAD potentiates ATP-induced P2X$_7$R activation in HEK293 cells coexpressing ART2 and P2X$_7$R. HEK293 cells stably transfected with WT murine P2X$_7$R (HEK-mP2X$_7$ cells) were used in all experiments. In experiments for *A–D*, the cells were transiently cotransfected with murine ART2.2 24 h before analysis of P2X$_7$R-dependent Ca^{2+} influx. In experiments for *E* and *F*, the HEK-mP2X$_7$ cells that lack ART2.2 expression were directly assayed. Cytosolic Ca^{2+} was measured in fura-2-loaded HEK cell suspensions as described in Fig. 3. The cell suspensions were pretreated with a mixture of 50 μM ADP and 50 μM UTP to activate and desensitize P2Y receptors 5 min before P2X$_7$R stimulation by the indicated concentrations of ATP; where indicated (as in the traces shown in *B*), 100 μM NAD (plus ADP-R) was also added 5 min prior to the addition of ATP. In each assay, the cells were permeabilized with digitonin (Digi) for the calibration of Ca^{2+}-dependent fura-2 fluorescence. *A* and *B*, ATP-induced Ca^{2+} influx without (*A*) or with (*B*) NAD pretreatment for 5 min. These traces are representative of observations from four experiments. *C* and *D*, Changes in cytosolic Ca^{2+} in ART2.2-transfected cells were quantified at 30 s (*C*) or 3 min (*D*) after the addition of the indicated concentrations of ATP with or without NAD pretreatment. Data bars represent the mean ± SE from four experiments. *E* and *F*, Identical experiments as in *C* and *D*, but with HEK-mP2X$_7$ cells not transfected with ART2.2. Data bars represent the mean ± SE from three experiments.

the HEK293 cells expressing P2X$_7$R but not ART2.2 (Fig. 4, *B*, *E*, and *F*).

These experiments focused on defining changes in P2X$_7$R activation by [ATP] in the threshold-to-EC$_{50}$ range because we (16) and others (2, 15) have noted that the conventional analysis of ATP concentration-response relationships for recombinant or native P2X$_7$R is complicated by the following: 1) the unusually high ATP EC$_{50}$ (~1 mM); 2) the allosteric effects of extracellular Mg^{2+} and Ca^{2+} on P2X$_7$R activity; and 3) the strong chelation of divalent cations by ATP (a divalent anion at physiological pH and ionic strength), such that the extracellular concentrations of free Mg^{2+} and free Ca^{2+} are decreased as the concentration of added ATP is increased to supramillimolar levels. The assay of Ca^{2+} influx as a sensitive and convenient readout of P2X$_7$R channel gating is further convoluted by the decreased extracellular [Ca^{2+}] and the consequent reduction in the chemical driving force at the supramillimolar [ATP]. Because the contribution of these various complicating factors is minimized at submillimolar [ATP], we assayed changes in threshold ATP concentrations rather than changes in the ATP EC$_{50}$ as the simplest index of increased ATP potency at the ADP-ribosylated P2X$_7$R.

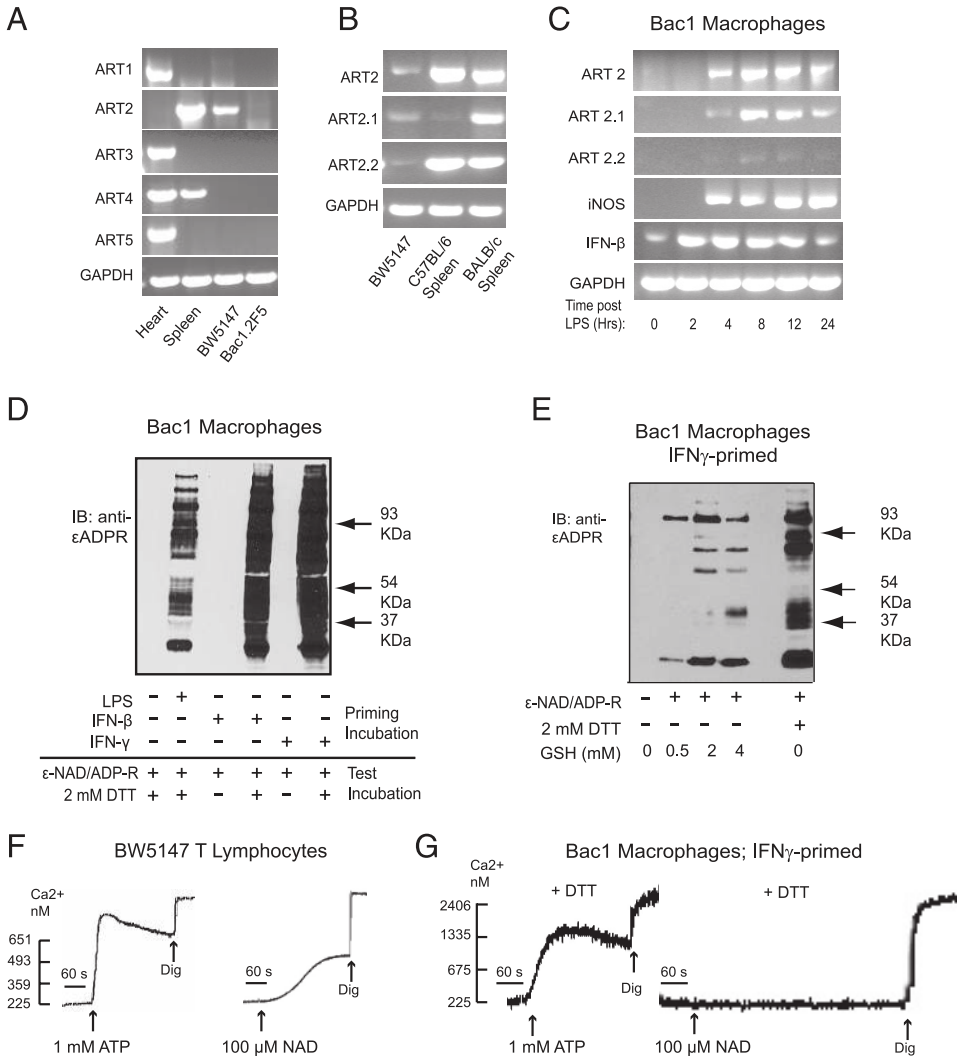

FIGURE 5. Differential effects of NAD/ART2 on $P2X_7R$ function in established murine macrophage and T lymphocyte cell lines. *A*, Expression of ART1, ART2, ART3, ART4, or ART5 mRNA was assayed by RT-PCR in BW5147 lymphocytes and Bac1.2F5 macrophages, as well as in freshly isolated extracts of heart or spleen from a BALB/c mouse. *B*, RT-PCR analysis for total ART2, ART2.1, and ART2.2 in BW5147 cells and freshly isolated spleen tissues from BALB/c or C57BL/6 mice. *C*, Bac1.2F5 macrophages were transferred to M-CSF-free medium and stimulated with LPS (100 ng/ml) for the indicated times before extraction and RT-PCR analysis for ART2, ART2.1, ART2.2, inducible NO synthase (iNOS), IL-1β, or GAPDH content. *D*, Bac1.2F5 macrophages were transferred to M-CSF-free medium and stimulated with or without IFN-β (100 U/ml), IFN-γ (100 U/ml), or LPS (100 ng/ml) for 24 h (priming incubation). The primed cells were then stimulated with 50 μM ε-NAD and 1 mM ADP-R in the presence or absence of 2 mM DTT at 37°C for 15 min (test incubation) before extraction for SDS-PAGE and Western blot analysis of 1G4-reactive, εADP-ribosylated proteins. IB, Immunoblotting. *E*, Bac1.2F5 macrophages were stimulated with or without IFN-γ (100 U/ml) for 24 h. The primed cells were then stimulated with 50 μM ε-NAD and 1 mM ADP-R in the presence or absence of the indicated concentrations of GSH or DTT at 37°C for 15 min. *F* and *G*, ATP- or NAD-induced changes in Ca^{2+} were assayed in fura-2-loaded suspensions of untreated BW5147 T lymphocytes (*F*) or Bac1.2F5 macrophages primed for 24 h with IFN-γ (*G*). For Bac1 cells, the 100 μM NAD was added together 1 mM ADP-R and 1 mM DTT. These results are representative of observations from three or more experiments.

Differential effects of NAD/ART2 on $P2X_7R$ function in established murine macrophage and T lymphocyte cell lines

The observation that NAD treatment decreased the threshold ATP concentration for heterologously expressed $P2X_7R$ in HEK293 suggested that NAD/ART2.1 might similarly regulate natively expressed $P2X_7R$ in murine macrophages. To facilitate these studies, we first determined that established murine macrophage and T cell lines were appropriate models for mechanistic analysis of the differential effects of NAD/ART2 on $P2X_7R$ function in primary murine macrophages vs T cells. We tested two murine macrophage cell lines (Bac1.2F5 and RAW264.7) and a murine T lymphoma cell line (BW5147). As in primary BMDM (36), the Bac1.2F5 macrophages (Fig. 5*A*) and RAW264.7 macrophages (data not shown) lacked basal expression of any ecto-ART subtypes at the mRNA level (heart or spleen extracts from BALB/c mice were used as positive control sources of ART1, ART2, ART3, ART4, and ART5 transcripts). However, Bac1.2F5 cells stimulated with 100 ng/ml LPS for 2–24 h selectively accumulated ART2.1 mRNA (Fig. 5*C*), and this up-regulation of ART2.1 correlated with increased expression of iNOS and IFN-β, two other LPS-inducible gene products. Thiol-dependent ART enzyme activity in intact Bac1.2F5 macrophages was detected using the 1G4 mAb-based Western blot assay (Fig. 5*D*). Multiple cell surface proteins were ADP-ribosylated in a strictly DTT-dependent manner in Bac1.2F5 macrophages primed by LPS, IFN-γ, or IFN-β to up-regulate ART2.1 expression (Fig. 5*D*). Extracellular GSH, a physiological

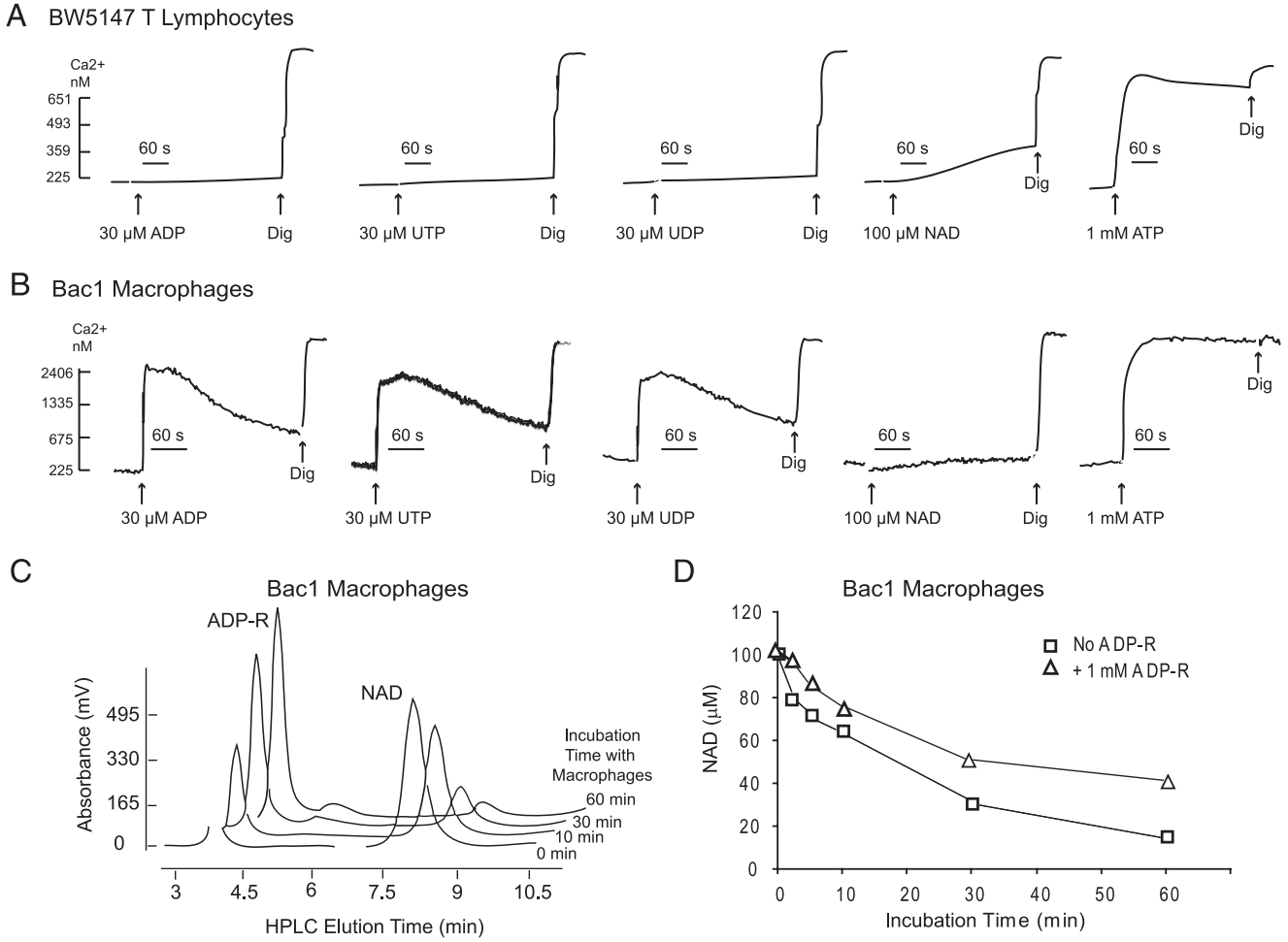

FIGURE 6. P2Y receptor-based Ca^{2+} signaling and extracellular NAD metabolism in murine macrophage and T lymphocyte cell lines. *A* and *B*, Cytosolic Ca^{2+} was assayed in fura-2-loaded suspensions of BW5147 T cells (*A*) or IFN-γ-primed Bac1.2F5 macrophages (*B*) challenged with the indicated concentrations of ADP, UTP, UDP, NAD, or ATP. The results are representative of observations from two experiments. Dig, Digitonin. *C* and *D*, Monolayers of Bac1.2F5 macrophages (10^6 cells/well in 6-well dishes) were incubated in 1 ml of BSS at 37°C supplemented with 100 μM NAD in the presence or absence of 1 mM ADP-R. At selected times (0–60 min), 100-μl aliquots of the extracellular medium were removed and processed for HPLC analysis. *C*, Stacked HPLC chromatograms of extracellular samples taken at the 0-, 10-, 30-, and 60-min time points. *D*, NAD concentrations at the indicated times were calculated from the HPLC chromatograms.

thiol reductant, also supported the ADP-ribosylation of multiple surface proteins in the IFN-primed macrophages (Fig. 5*E*). Similarly as primary spleen T cells from BALB/c mice, BW5147 T lymphoma cells constitutively expressed both ART2.1 and ART2.2 mRNA (Fig. 5, *A* and *B*) and also expressed functional ART2 activity as detected by the 1G4 mAb assay (data not shown). Splenic T cells from C57BL/6 mice expressed ART2.2, but not ART2.1, at significant levels. Notably, the BW5147 T cells also exhibited robust Ca^{2+} influx responses to either ATP or NAD (Fig. 5*F*) as observed in primary splenic lymphocytes (Fig. 1, *A* and *B*). In contrast, IFN-γ-primed Bac1.2F5 macrophages responded to exogenous ATP, but not to NAD alone (Fig. 5*G*), similarly as IFN- or LPS-primed primary BMDM (Fig. 1*D*).

Recent studies have indicated that extracellular NAD also activates some subtypes of G protein-coupled P2Y nucleotide receptors that can trigger mobilization of intracellular Ca^{2+} stores (48). The Ca^{2+} influx-based assay used to monitor P2X$_7$R activity required prestimulation of the macrophages with a mixture of ADP and UTP to first activate and desensitize the Ca^{2+}-mobilizing P2Y1, P2Y2, and P2Y6 receptors expressed in these cells (41, 42). We tested the possibility that this protocol also desensitized NAD-reactive P2Y receptors that might be expressed in T cells and macrophages. BW5147 and Bac1.2F5 macrophages were stimulated with only single-nucleotide agonists with no prior desensitization incubation. Although murine T cells have been reported to express mRNA for various P2Y receptor subtypes (14), we observed no Ca^{2+}-mobilizing responses to micromolar concentrations of ADP (P2Y1 agonist), UTP (P2Y2/P2Y4 agonist), or UDP (P2Y6 agonist) in the BW5147 T cells (Fig. 6*A*). Moreover, primary T cells from P2X$_7$R-knockout mice showed no Ca^{2+} response to ATP or NAD (Fig. 1). Thus, naive murine T cells do not express functionally significant levels of Ca^{2+}-mobilizing P2Y receptors that can be activated by ATP, ADP, UTP, UDP, or NAD. In contrast, Bac1 macrophages, like primary murine BMDM (36), exhibited strong Ca^{2+} mobilization responses to ADP, UTP, and UDP, but not to NAD (Fig. 6*B*). Thus, the differential responses of T cells vs macrophages to NAD do not involve obvious roles for NAD-sensitive P2Y receptor subtypes.

Other ectoenzymes that modulate the efficiency of NAD-dependent ADP-ribosylation of cell surface proteins can also be differentially expressed in leukocyte subsets. These include the CD38 NAD-glycohydrolases and CD203 nucleotide pyrophosphatases that metabolize extracellular NAD and thereby reduce

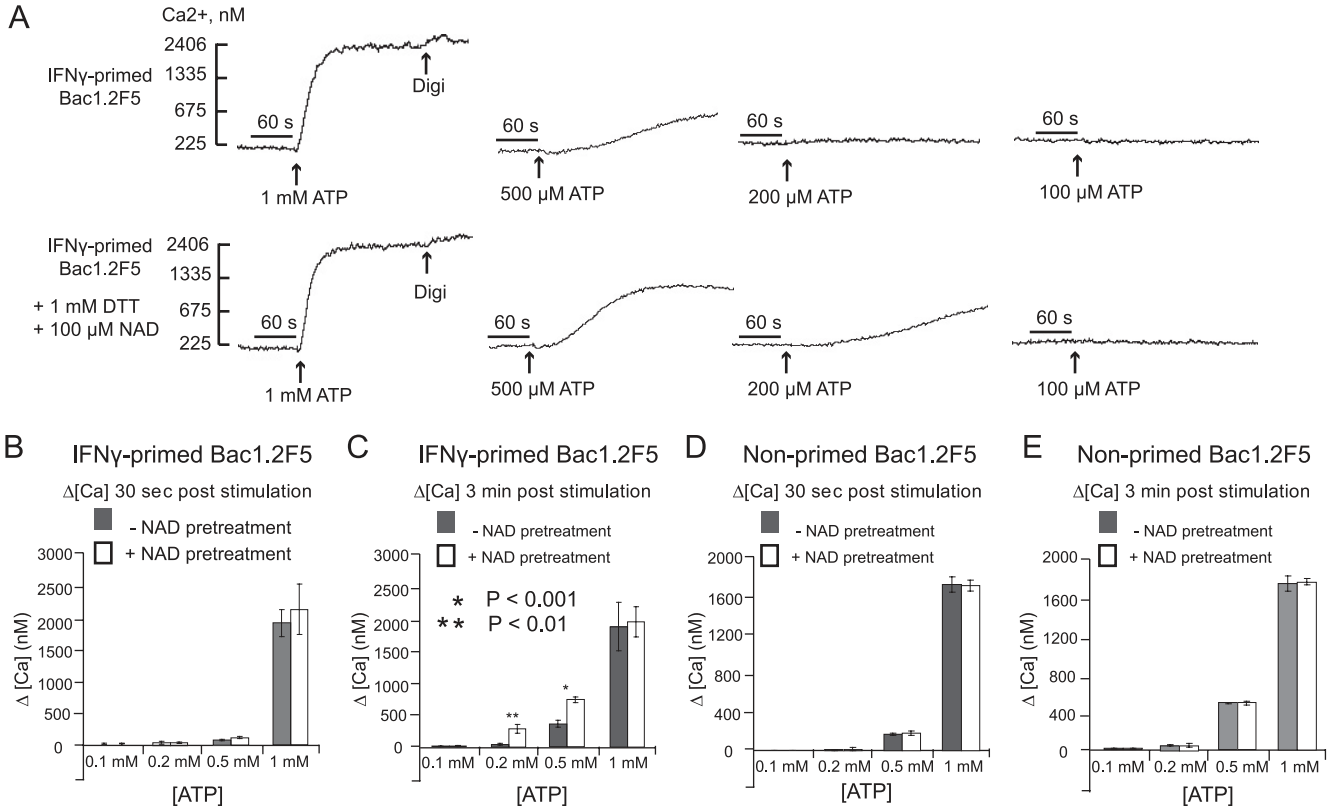

FIGURE 7. NAD potentiates ATP-induced $P2X_7R$ activation in IFN-primed murine macrophages that express ART2.1. Bac1.2F5 macrophages were transferred to M-CSF-free medium and then stimulated with IFN-γ (100 U/ml) for 24 h (*A–C*) or were incubated in M-CSF-free medium for 24 h in the absence of IFN-γ (*D* and *E*). Cytosolic Ca^{2+} was measured in fura-2-loaded Bac1 cell suspensions as previously described but with the inclusion of 1 mM DTT and 1 mM ADP-R in all test media. The cell suspensions were pretreated with a mixture of 50 μM ADP and 50 μM UTP to activate and desensitize P2Y receptors 5 min before $P2X_7R$ stimulation by the indicated concentrations of ATP; where indicated (as in the traces shown in *A*), 100 μM NAD was also added 5 min prior to the addition of ATP. In each assay, the cells were permeabilized with digitonin (Digi) for calibration of Ca^{2+}-dependent fura-2 fluorescence. *A*, ATP-induced Ca^{2+} influx without or with NAD pretreatment for 5 min. These traces are representative of observations from four experiments. *B* and *C*, Changes in cytosolic Ca^{2+} in IFN-γ-primed Bac1 macrophages were quantified at 30 s (*B*) or 3 min (*C*) after the addition of the indicated concentrations of ATP with or without NAD pretreatment. Data bars represent the mean ± SE from four experiments. *D* and *E*, Identical experiments to those in *B* and *C*, but with Bac1 macrophages that were not primed with IFN-γ. Data bars represent the mean ± SE from four experiments.

substrate drive to the ARTs (26). We used HPLC analyses to test whether the inability of NAD per se to trigger Ca^{2+} influx or mobilization in murine macrophages was due to very rapid metabolism of the added extracellular NAD. Although Bac1 macrophages metabolized 100 μM NAD to ADP-R, the $t_{1/2}$ for this reaction was ~20 min, such that >50 μM NAD was present throughout the 1–10 min test periods used to assay Ca^{2+} influx/mobilization responses (Fig. 6*C*). Inclusion of exogenous ADP-R (routinely added to maintain ADP-ribosylation of target proteins) further slowed the rate of NAD clearance. Thus, excessive NAD catabolism is an unlikely reason for the differential responses of macrophages vs T cells to extracellular NAD.

NAD potentiates ATP-induced $P2X_7R$ activation in murine macrophages and T lymphocytes

IFN-γ-primed Bac1.2F5 macrophages were briefly pretreated with NAD in the presence of DTT to allow ADP-ribosylation of cell surface proteins and then challenged with various doses of ATP to trigger $P2X_7R$-dependent Ca^{2+} influx. Similar to its effects in ART2/$P2X_7$-transfected HEK293 cells, NAD pretreatment increased the sensitivity of the IFN-primed Bac1 macrophages to submillimolar ATP (Figs. 7, *A–C*). In contrast, naive Bac1.2F5 cells, which were not primed with IFN-γ and thus lacked expression of ART2.1, did not exhibit the NAD-dependent increase in ATP sensitivity (Figs. 7, *D* and *E*). Additional experiments demonstrated that NAD pretreatment produced similar increases in ATP sensitivity in other murine macrophage models, including IFN-β-primed RAW264.7 macrophages (Fig. 8*A*) and IFN-γ-primed BALB/c primary BMDM (Fig. 8*B*). Similarly as Bac1.2F cells (Fig. 5) and primary BMDM (36), the RAW264.7 macrophage line exhibited up-regulation of ART2.1 mRNA and thiol-dependent ecto-ART activity in response to IFN-β stimulation (data not shown).

NAD pretreatment also increased the sensitivity to ATP in the BW5147 T lymphocytes. These experiments involved stimulation of these cells with submaximally active concentrations of NAD (10 μM) and/or ATP (300 μM). Notably, when combined, 10 μM NAD and 300 μM ATP acted synergistically to increase $P2X_7R$-mediated Ca^{2+} influx (Fig. 8*C*).

ART2 can use dinucleotide substrates other than NAD to covalently ribosylate arginine residues in target proteins; these alternative substrates include ε-NAD and nicotinamide guanine dinucleotide (NGD). We previously reported that ribosylation of the $P2X_7R$ by ε-NAD or NGD in primary murine T cells does not stimulate the receptor but rather antagonizes NAD-induced receptor activation (20). We observed similar effects of ε-NAD on $P2X_7R$ function in the BW5147 T cell line (Figs. 9, *A* and *B*). Notably, $P2X_7$ receptors ribosylated by εNAD also have decreased sensitivity to activation by submaximal ATP as shown in primary

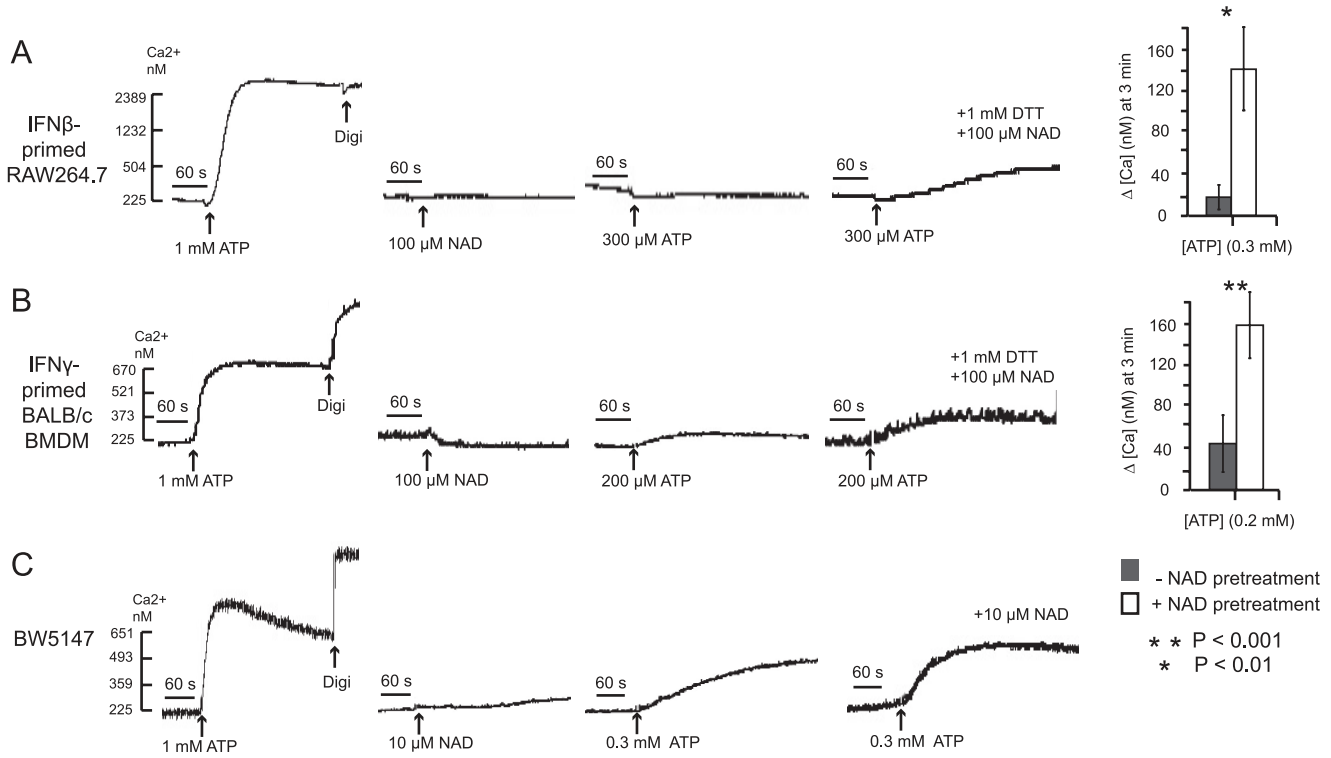

FIGURE 8. Comparative effects of NAD on the potentiation of ATP-induced P2X$_7$R activation in primary macrophages, a macrophage cell line, and a T cell line. Experiments similar to those described in Fig. 6 with Bac1.2F5 macrophages were performed using other murine leukocytes that express P2X$_7$R. *A*, RAW264.7 macrophages were transferred to M-CSF-free medium and stimulated with IFN-β (100 U/ml) for 24 h. The primed macrophages were stimulated with 1 mM ATP alone, 100 μM NAD (plus DTT) alone, or with 300 μM ATP in the absence or presence of a pretreatment with 100 μM NAD (plus DTT) for 5 min. The accompanying histograms (mean ± SE from three experiments) show the quantified changes in Ca^{2+} at 3 min after the addition of 300 μM ATP with and without NAD pretreatment. *B*, BALB/c BMDM were transferred to M-CSF-free medium and stimulated with IFN-γ (100 U/ml) for 24 h. The cells were stimulated and assayed as described in *A*, but with 200 μM ATP as the test pulse. The accompanying histograms (mean ± SE from three experiments) show the quantified changes in Ca^{2+} 3 min after the addition of 200 μM ATP with and without NAD pretreatment. *C*, BW5147 T lymphocytes were stimulated with 1 mM ATP alone, 10 μM NAD alone, or 300 μM ATP in the absence or presence of a pretreatment with 10 μM NAD for 5 min. These results are representative of observations from three experiments.

murine T cells (20), BW5147 T lymphoma cells (Figs. 9, *A* and *B*), IFN-γ-primed Bac1.2F5 macrophages (Fig. 9*C*), and IFN-β-primed RAW264.7 macrophages (Fig. 9*D*).

NAD potentiates ATP-induced P2X$_7$R-dependent pore formation in murine macrophages

The previous data showing that ADP-ribosylation of P2X$_7$R potentiates ATP activation of these receptors in murine macrophages and HEK293 cells used increases in cytosolic Ca^{2+} as a sensitive readout of P2X$_7$R channel activity. We considered the possibility that the P2Y prestimulation protocol (used to desensitize Ca^{2+}-mobilizing P2Y receptors) triggered G protein-coupled signaling pathways that modulate the functional interactions between ART2 and P2X$_7$R in macrophages and HEK293 cells. Thus, we measured the effects of NAD/ART2 on nonselective pore formation as an alternative readout of P2X$_7$R activation that does not require prestimulation and desensitization of P2Y receptors. Pore formation was assayed by ethidium accumulation in IFN-γ-primed (Fig. 10*A*) vs control (Fig. 10*B*) Bac1.2F5 macrophages, similar to the YO-PRO-1 accumulation assay previously described for HEK293 cells (Fig. 3*D*). NAD (plus DTT) by itself did not stimulate ethidium accumulation but did increase the rate of accumulation triggered by submillimolar ATP in the IFN-γ primed, but not control, Bac1 macrophages. Notably, the potentiating effects of NAD on ethidium influx were observed at a higher range of extracellular ATP concentrations (0.5–1 mM) than the effects on Ca^{2+} influx (0.1–0.5 mM ATP; Fig. 7). This is consistent with the fact that ethidium influx is a secondary response to P2X$_7$R stimulation (49) that involves gating of pannexin-1 hemichannels (4). Previous studies have indicated that the ATP concentration-response relationship describing this secondary response is right shifted relative to the concentration-response relationship describing the primary gating of P2X$_7$R channels (2, 50).

Discussion

From the initial functional characterization of the permeabilizing "P2Z" ATP receptor 30 years ago (51–53), through the molecular identification of the P2Z receptor phenotype as the product of the P2X$_7$R gene (2), and up to the most recent analyses of in vivo functional deficits in P2X$_7$-knockout mice (10, 11, 54), two fundamental and perplexing questions regarding the P2X$_7$R have been repeatedly considered. First, why does this particular ATP receptor, in sharp contrast to the six other P2X receptor subtypes, require millimolar levels of extracellular ATP for activation when studied in isolated cells? This unusual characteristic suggests that low affinity variants of an ancestral P2X$_7$R were favored by positive selection as the receptor acquired its physiological roles as a regulator of proinflammatory signaling and cell death. Low ATP affinity prevents inadvertent activation of these highly consequential but poorly reversible responses until leukocytes accumulate at sites of tissue damage or microbial invasion. However, this raises a second and corollary question: how does the P2X$_7$R become activated in leukocytes within these latter tissue compartments given the receptor's low affinity of ATP? Recent studies support three possible mechanisms that are not mutually exclusive: 1)

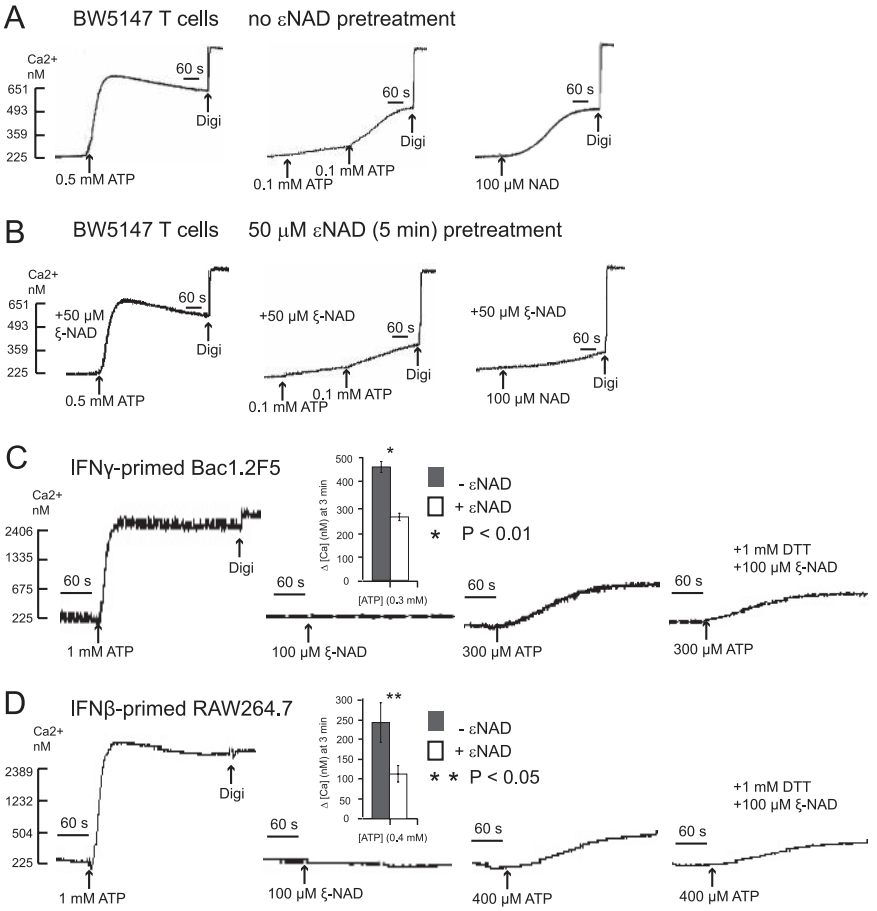

FIGURE 9. ε-NAD, an NAD analog, desensitizes $P2X_7R$ to ATP in macrophages and T lymphocytes. Experiments similar to those described in Fig. 7 were performed but used the NAD analog, εNAD, as the ART2 substrate for the pretreatment of murine leukocytes that express $P2X_7R$. *A*, BW5147 T lymphocytes were stimulated with 0.5 mM ATP alone, 200 μM ATP alone (added as two sequential 100 μM pulses), or 100 μM NAD alone. These results are representative of observations from two experiments. *B*, Identical experiment as in *A* but with BW5147 T lymphocytes that were pretreated with 50 μM εNAD for 5 min before stimulation with 0.5 mM ATP alone, 200 μM ATP alone (added as two sequential 100 μM pulses), or 100 μM NAD alone. These results are representative of observations from two experiments. Digi, Digitonin. *C*, Bac1.2F5 macrophages were transferred to M-CSF-free medium and stimulated with IFN-γ (100 U/ml) for 24 h. The primed macrophages were acutely stimulated with 1 mM ATP alone, 100 μM εNAD (plus DTT) alone, or 300 μM ATP in the absence or presence of a pretreatment with 100 μM εNAD (plus DTT) for 5 min. The accompanying histograms (mean ± SE from three experiments) show the quantified changes in Ca^{2+} at 3 min after the addition of 300 μM ATP with and without εNAD pretreatment. *D*, RAW264.7 macrophages were transferred to M-CSF-free medium and stimulated with IFN-β (100 U/ml) for 24 h. The primed macrophages were acutely stimulated with 1 mM ATP alone, 100 μM εNAD (plus DTT) alone, or 400 μM ATP in the absence or presence of a pretreatment with 100 μM εNAD (plus DTT) for 5 min. The accompanying histograms (mean ± SE from three experiments) show the quantified changes in Ca^{2+} at 3 min after the addition of 400 μM ATP with and without εNAD pretreatment.

highly localized accumulation of ATP for autocrine activation of $P2X_7R$ within diffusion-restricted cell surface compartments (12–14); 2) allosteric modulation of ATP affinity via conformational changes in $P2X_7$ trimeric channels produced by local biophysical conditions or covalent modification of the $P2X_7R$ protein itself (15, 16, 18, 19, 55, 56); and 3) the ATP-independent activation of $P2X_7R$ via conformational changes produced by ADP-ribosylation of key arginines within the extracellular loop of the $P2X_7R$ (20, 21, 57). The experiments described in this report provide new insights into the latter two regulatory mechanisms and additionally suggest that a fourth mechanism, one involving tissue/cell-selective expression of accessory molecules and/or of $P2X_7R$ splice variants, contributes to the regulation of $P2X_7R$ function.

The ability of NAD to drive the covalent modification of extracellular residues of the $P2X_7R$ comprises a novel mechanism to produce relatively long-lasting changes in the conformational state of these ligand-gated ion channels during transient increases in extracellular NAD, ATP, and other normally intracellular metabolites, such as lysolipids, that can regulate $P2X_7R$ function (22, 57, 58). Previous studies demonstrated that NAD can trigger $P2X_7R$ activation in murine T lymphocytes even when these cells were incubated in the presence of apyrase to scavenge any released ATP (20). Moreover, $P2X_7R$ activation was sustained in T cells briefly treated with NAD and then washed free of this nucleotide. In contrast, ATP-stimulated $P2X_7R$ rapidly deactivated when T cells were transferred to ATP-free medium. These findings indicate that ADP-ribosylation of $P2X_7R$ subunits in murine T cells induces a conformational change sufficient to gate the opening of these trimeric channels even in the absence of ATP binding. However, our studies of $P2X_7R$ function in murine macrophages and HEK293 cells indicate that this ATP-independent activation of $P2X_7R$ by ADP-ribosylation is not a general mode of $P2X_7R$ regulation but rather reflects the specialized conditions present in murine T lymphocytes.

Notably, although NAD by itself was able to gate $P2X_7R$ in NZW T lymphocytes expressing solely ART2.1, it failed to activate $P2X_7R$ either in murine macrophages that coexpress native $P2X_7R$ and ART2.1 or in HEK293 cells engineered to coexpress

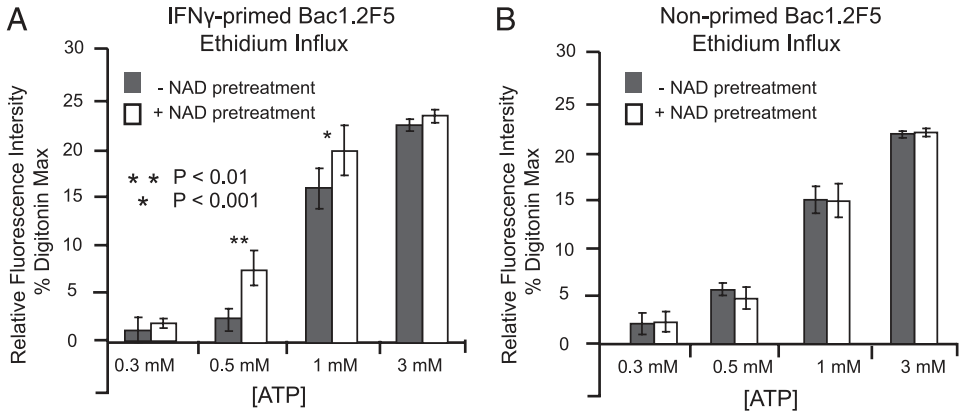

FIGURE 10. NAD potentiates ATP-induced pore formation in IFN-γ-primed murine macrophages. Bac1.2F5 macrophages were suspended in BSS, and ATP-induced ethidium accumulation was assayed as described in *Materials and Methods*. Bac1.2F5 macrophages were transferred to M-CSF-free medium and stimulated with (*A*) or without (*B*) IFN-γ (100 U/ml) for 24 h before an assay of ethidium accumulation. The primed macrophages were stimulated with the indicated concentrations of ATP in the absence or presence of pretreatment with 100 μM NAD (plus 1 mM DTT) for 5 min before the addition of ATP. Accumulation of fluorescent ethidium/DNA/RNA complexes was measured at 350 s after ATP addition. Data bars represent the mean ± SE from four experiments.

murine P2X$_7$R and murine ART2 ectoenzymes. However, NAD acted synergistically with ATP to regulate P2X$_7$R in both the macrophages and the engineered HEK cells, and this effect of NAD was strictly dependent on the expression of ART2.1 or ART2.2 in both cell models. How can these regulatory effects of NAD/ART2 on ATP-dependent P2X$_7$R activation observed in murine macrophages and HEK293 cells be reconciled with the robust ATP-independent activation by NAD/ART2 in murine T cells? Possible explanations for the difference in P2X$_7$R signaling observed between myeloid and lymphoid cells are that T cells, but not macrophages or HEK cells, express other regulatory proteins that facilitate the ATP-independent gating of P2X$_7$R in response to ADP-ribosylation, or that the local membrane microenvironments containing P2X$_7$R and ART2 are different in the two cell types. Another possible explanation might be the expression of different, recently identified splice variants of rodent P2X$_7$R in T cells vs macrophages. Indeed, Taylor et al. have recently reported that P2X$_7$R function is preserved in the T lymphocytes, but not in macrophages, from one strain of P2X$_7$-null mice that was generated by lacZ insertion into exon 1 of the *p2rx7* gene (59). Determining whether different murine tissues and cells, particularly hematopoietic cell types, express splice variants of the P2X$_7$R with altered functional responses to ART2-mediated modification is an important goal for future experiments.

It is important to consider how ADP-ribosylation of key Arg residues may affect the conformation of these trimeric channels. Electrophysiological analyses of P2X-family channels at the whole cell and single-channel levels indicate that at least two, and probably three, molecules of ATP need to be bound per channel for optimal gating (9, 60). Moreover, the critical ATP binding sites appear to be formed at the interfaces between the extracellular loops of individual subunits, rather than within each subunit loop as initially hypothesized (61, 62). In this regard, the covalently associated ADP-R at Arg^{125} of a P2X$_7$ subunit may interact with the key interfacial amino residues that form the ATP-binding site. However, ADP-R is larger than ATP per se, and it is unclear whether the P2X$_7$R channel complex can accommodate ADP-ribosylation of all three subunits or whether only one or two subunits per channel can be efficiently modified. Differences in the number of covalently modified subunits per channel, due possibly to steric hindrance, may underlie the distinctive consequences of NAD/ART2 action on P2X$_7$R function in macrophages vs T cells. ADP-ribosylation of these receptors in macrophages may be limited to only one or two subunits per channel, which is insufficient for gating but sufficient for positive allosteric action at the remaining interfacial ATP-binding sites. This would be consistent with the observed increase in potency of ATP at P2X$_7$R in ART2.1-expressing macrophages (or HEK293 cells) pretreated with NAD. In contrast, the predominant P2X$_7$R channels in T cells or the mutant P2X$_7$R-R276K channels in HEK cells may have conformations that accommodate and permit ADP-ribosylation of all three subunits.

It is currently unclear whether ADP-ribosylation is a common mechanism for the activation or sensitization of P2X$_7$R signaling in other tissues or organisms. Notably, the Arg^{125} and Arg^{133} residues are conserved in the human P2X$_7$R (63), but the human ART2A and ART2B loci are transcriptionally silent pseudogenes (26, 64). Thus, human T cells and macrophages lack the capacity for *cis*-regulation of P2X$_7$R by a coexpressed ecto-ART. However, human ART1 is constitutively expressed in neutrophils, and this GPI-anchored enzyme is rapidly shed during neutrophil activation in response to bacterial infection (65). ART1 is also expressed by human airway epithelial cells basally and at increased levels in response to bacterial mediators (66–68). Thus, the P2X$_7$R in human macrophages and T cells might be *trans*-regulated by shed ART1 that accumulates at sites of bacterial infection and neutrophil recruitment. Such a mechanism may also be operative in mice that also express ART1 in other tissues such as cardiac and skeletal muscle (69).

NAD is released to extracellular environments during the early stage of inflammatory response (57). Besides its ability to trigger P2X$_7$R-dependent T cell death (20), extracellular NAD has been reported as an agonist for P2Y11 receptors in human granulocytes (48). Our study now shows that NAD also increases the sensitivity of the P2X$_7$R to ATP gating in macrophages. This action of NAD requires expression of the thiol-sensitive ART2.1 enzymes and reduced thiols, such as glutathione and cysteine, that can accumulate at inflammatory loci due to release from activated macrophages and the hypoxia that often characterizes such loci (31). We have found that ART2.1 is widely expressed in other leukocytes, such as dendritic cells and B lymphocytes (70). Thus, the sensitization of ATP-dependent P2X$_7$R activation by NAD/ART2.1 may provide an additional layer of regulatory control in multiple phases of innate and adaptive immunity.

Disclosures

The authors have no financial conflict of interest.

References

1. North, R. A. 2002. Molecular physiology of P2X receptors. *Physiol. Rev.* 82: 1013–1067.
2. Surprenant, A., F. Rassendren, E. Kawashima, R. A. North, and G. Buell. 1996. The cytolytic P2Z receptor for extracellular ATP identified as a P2X receptor ($P2X_7$). *Science* 272: 735–738.
3. Nicke, A. 2008. Homotrimeric complexes are the dominant assembly state of native $P2X_7$ subunits. *Biochem. Biophys. Res. Commun.* 377: 803–808.
4. Pelegrin, P., and A. Surprenant. 2006. Pannexin-1 mediates large pore formation and interleukin-1β release by the ATP-gated $P2X_7$ receptor. *EMBO J.* 25: 5071–5082.
5. Lister, M. F., J. Sharkey, D. A. Sawatzky, J. P. Hodgkiss, D. J. Davidson, A. G. Rossi, and K. Finlayson. 2007. The role of the purinergic $P2X_7$ receptor in inflammation. *J. Inflamm.* (*Lond.*) 4: 5.
6. Ferrari, D., C. Pizzirani, E. Adinolfi, R. M. Lemoli, A. Curti, M. Idzko, E. Panther, and F. Di Virgilio. 2006. The $P2X_7$ receptor: a key player in IL-1 processing and release. *J. Immunol.* 176: 3877–3883.
7. Di Virgilio, F., and J. S. Wiley. 2002. The $P2X_7$ receptor of CLL lymphocytes–a molecule with a split personality. *Lancet* 360: 1898–1899.
8. Dubyak, G. R. 2007. Go it alone no more–$P2X_7$ joins the society of heteromeric ATP-gated receptor channels. *Mol. Pharmacol.* 72: 1402–1405.
9. Khakh, B. S., and R. A. North. 2006. P2X receptors as cell-surface ATP sensors in health and disease. *Nature* 442: 527–532.
10. Chessell, I. P., J. P. Hatcher, C. Bountra, A. D. Michel, J. P. Hughes, P. Green, J. Egerton, M. Murfin, J. Richardson, W. L. Peck, et al. 2005. Disruption of the $P2X_7$ purinoceptor gene abolishes chronic inflammatory and neuropathic pain. *Pain* 114: 386–396.
11. Ke, H. Z., H. Qi, A. F. Weidema, Q. Zhang, N. Panupinthu, D. T. Crawford, W. A. Grasser, V. M. Paralkar, M. Li, L. P. Audoly, et al. 2003. Deletion of the $P2X_7$ nucleotide receptor reveals its regulatory roles in bone formation and resorption. *Mol. Endocrinol.* 17: 1356–1367.
12. Netea, M. G., C. A. Nold-Petry, M. F. Nold, L. A. Joosten, B. Opitz, J. H. van der Meer, F. L. van de Veerdonk, G. Ferwerda, B. Heinhuis, I. Devesa, et al. 2009. Differential requirement for the activation of the inflammasome for processing and release of IL-1β in monocytes and macrophages. *Blood* 113: 2324–2335.
13. Piccini, A., S. Carta, S. Tassi, D. Lasiglie, G. Fossati, and A. Rubartelli. 2008. ATP is released by monocytes stimulated with pathogen-sensing receptor ligands and induces IL-1β and IL-18 secretion in an autocrine way. *Proc. Natl. Acad. Sci. USA* 105: 8067–8072.
14. Schenk, U., A. M. Westendorf, E. Radaelli, A. Casati, M. Ferro, M. Fumagalli, C. Verderio, J. Buer, E. Scanziani, and F. Grassi. 2008. Purinergic control of T cell activation by ATP released through pannexin-1 hemichannels. *Sci. Signal.* 1: ra6.
15. Michel, A. D., I. P. Chessell, and P. P. Humphrey. 1999. Ionic effects on human recombinant $P2X_7$ receptor function. *Naunyn Schmiedebergs Arch. Pharmacol.* 359: 102–109.
16. Verhoef, P. A., S. B. Kertesy, K. Lundberg, J. M. Kahlenberg, and G. R. Dubyak. 2005. Inhibitory effects of chloride on the activation of caspase-1, IL-1β secretion, and cytolysis by the $P2X_7$ receptor. *J. Immunol.* 175: 7623–7634.
17. Riedel, T., G. Schmalzing, and F. Markwardt. 2007. Influence of extracellular monovalent cations on pore and gating properties of $P2X_7$ receptor-operated single-channel currents. *Biophys. J.* 93: 846–858.
18. Michel, A. D., and E. Fonfria. 2007. Agonist potency at $P2X_7$ receptors is modulated by structurally diverse lipids. *Br. J. Pharmacol.* 152: 523–537.
19. Takenouchi, T., Y. Iwamaru, S. Sugama, M. Sato, M. Hashimoto, and H. Kitani. 2008. Lysophospholipids and ATP mutually suppress maturation and release of IL-1β in mouse microglial cells using a Rho-dependent pathway. *J. Immunol.* 180: 7827–7839.
20. Seman, M., S. Adriouch, F. Scheuplein, C. Krebs, D. Freese, G. Glowacki, P. Deterre, F. Haag, and F. Koch-Nolte. 2003. NAD-induced T cell death: ADP-ribosylation of cell surface proteins by ART2 activates the cytolytic $P2X_7$ purinoceptor. *Immunity* 19: 571–582.
21. Adriouch, S., P. Bannas, N. Schwarz, R. Fliegert, A. H. Guse, M. Seman, F. Haag, and F. Koch-Nolte. 2008. ADP-ribosylation at R125 gates the $P2X_7$ ion channel by presenting a covalent ligand to its nucleotide binding site. *FASEB J.* 22: 861–869.
22. Haag, F., S. Adriouch, A. Brass, C. Jung, S. Moller, F. Scheuplein, P. Bannas, M. Seman, and F. Koch-Nolte. 2007. Extracellular NAD and ATP: partners in immune cell modulation. *Purinergic Signal.* 3: 71–81.
23. Bortell, R., T. Kanaitsuka, L. A. Stevens, J. Moss, J. P. Mordes, A. A. Rossini, and D. L. Greiner. 1999. The RT6 (Art2) family of ADP-ribosyltransferases in rat and mouse. *Mol. Cell. Biochem.* 193: 61–68.
24. Sardinha, D. F., and T. V. Rajan. 1999. *cis*-Acting regulation of splenic Art2 gene expression in inbred mouse strains. *Immunogenetics* 49: 700–703.
25. Koch-Nolte, F., T. Duffy, M. Nissen, S. Kahl, N. Killeen, V. Ablamunits, F. Haag, and E. H. Leiter. 1999. A new monoclonal antibody detects a developmentally regulated mouse ecto-ADP-ribosyltransferase on T cells: subset distribution, inbred strain variation, and modulation upon T cell activation. *J. Immunol.* 163: 6014–6022.
26. Seman, M., S. Adriouch, F. Haag, and F. Koch-Nolte. 2004. Ecto-ADP-ribosyltransferases (ARTs): emerging actors in cell communication and signaling. *Curr. Med. Chem.* 11: 857–872.
27. Kawamura, H., T. Sugiyama, D. M. Wu, M. Kobayashi, S. Yamanishi, K. Katsumura, and D. G. Puro. 2003. ATP: a vasoactive signal in the pericyte-containing microvasculature of the rat retina. *J. Physiol.* 551: 787–799.
28. Aswad, F., H. Kawamura, and G. Dennert. 2005. High sensitivity of $CD4^+CD25^+$ regulatory T cells to extracellular metabolites nicotinamide adenine dinucleotide and ATP: a role for $P2X_7$ receptors. *J. Immunol.* 175: 3075–3083.
29. Hara, N., M. Terashima, M. Shimoyama, and M. Tsuchiya. 2000. Mouse T-cell antigen Rt6.1 has thiol-dependent NAD glycohydrolase activity. *J. Biochem.* 128: 601–607.
30. Yeh, M. W., M. Kaul, J. Zheng, H. S. Nottet, M. Thylin, H. E. Gendelman, and S. A. Lipton. 2000. Cytokine-stimulated, but not HIV-infected, human monocyte-derived macrophages produce neurotoxic levels of L-cysteine. *J. Immunol.* 164: 4265–4270.
31. Moriarty-Craige, S. E., and D. P. Jones. 2004. Extracellular thiols and thiol/disulfide redox in metabolism. *Annu. Rev. Nutr.* 24: 481–509.
32. Haag, F., D. Freese, F. Scheublein, W. Ohlrogge, S. Adriouch, M. Seman, and F. Koch-Nolte. 2002. T cells of different developmental stages differ in sensitivity to apoptosis induced by extracellular NAD. *Dev. Immunol.* 9: 197–202.
33. Ohlrogge, W., F. Haag, J. Lohler, M. Seman, D. R. Littman, N. Killeen, and F. Koch-Nolte. 2002. Generation and characterization of ecto-ADP-ribosyltransferase ART2.1/ART2.2-deficient mice. *Mol. Cell. Biol.* 22: 7535–7542.
34. Adriouch, S., W. Ohlrogge, F. Haag, F. Koch-Nolte, and M. Seman. 2001. Rapid induction of naive T cell apoptosis by ecto-nicotinamide adenine dinucleotide: requirement for mono(ADP-ribosyl)transferase 2 and a downstream effector. *J. Immunol.* 167: 196–203.
35. Kanaitsuka, T., R. Bortell, L. A. Stevens, J. Moss, D. Sardinha, T. V. Rajan, D. Zipris, J. P. Mordes, D. L. Greiner, and A. A. Rossini. 1997. Expression in BALB/c and C57BL/6 mice of Rt6-1 and Rt6-2 ADP-ribosyltransferases that differ in enzymatic activity: C57BL/6 Rt6-1 is a natural transferase knockout. *J. Immunol.* 159: 2741–2749.
36. Hong, S., A. Brass, M. Seman, F. Haag, F. Koch-Nolte, and G. R. Dubyak. 2007. Lipopolysaccharide. IFN-γ, and IFN-β induce expression of the thiol-sensitive ART2.1 ecto-ADP-ribosyltransferase in murine macrophages. *J. Immunol.* 179: 6215–6227.
37. Koch-Nolte, F., G. Glowacki, P. Bannas, F. Braasch, G. Dubberke, E. Ortolan, A. Funaro, F. Malavasi, and F. Haag. 2005. Use of genetic immunization to raise antibodies recognizing toxin-related cell surface ADP-ribosyltransferases in native conformation. *Cell. Immunol.* 236: 66–71.
38. Myers, A. J., B. Eilertson, S. A. Fulton, J. L. Flynn, and D. H. Canaday. 2005. The purinergic $P2X_7$ receptor is not required for control of pulmonary *Mycobacterium tuberculosis* infection. *Infect. Immun.* 73: 3192–3195.
39. Adriouch, S., G. Dubberke, P. Diessenbacher, F. Rassendren, M. Seman, F. Haag, and F. Koch-Nolte. 2005. Probing the expression and function of the $P2X_7$ purinoceptor with antibodies raised by genetic immunization. *Cell. Immunol.* 236: 72–77.
40. Humphreys, B. D., C. Virginio, A. Surprenant, J. Rice, and G. R. Dubyak. 1998. Isoquinolines as antagonists of the $P2X_7$ nucleotide receptor: high selectivity for the human versus rat receptor homologues. *Mol. Pharmacol.* 54: 22–32.
41. del Rey, A., V. Renigunta, A. H. Dalpke, J. Leipziger, J. E. Matos, B. Robaye, M. Zuzarte, A. Kavelaars, and P. J. Hanley. 2006. Knock-out mice reveal the contributions of P2Y and P2X receptors to nucleotide-induced $Ca2^+$ signaling in macrophages. *J. Biol. Chem.* 281: 35147–35155.
42. da Cruz, C. M., A. L. Ventura, J. Schachter, H. M. Costa-Junior, H. A. da Silva Souza, F. R. Gomes, R. Coutinho-Silva, D. M. Ojcius, and P. M. Persechini. 2006. Activation of ERK1/2 by extracellular nucleotides in macrophages is mediated by multiple P2 receptors independently of $P2X_7$-associated pore or channel formation. *Br. J. Pharmacol.* 147: 324–334.
43. Beigi, R. D., S. B. Kertesy, G. Aquilina, and G. R. Dubyak. 2003. Oxidized ATP (oATP) attenuates proinflammatory signaling via P2 receptor-independent mechanisms. *Br. J. Pharmacol.* 140: 507–519.
44. Schachter, J. B., S. M. Sromek, R. A. Nicholas, and T. K. Harden. 1997. HEK293 human embryonic kidney cells endogenously express the P2Y1 and P2Y2 receptors. *Neuropharmacology* 36: 1181–1187.
45. Qu, Y., L. Franchi, G. Nunez, and G. R. Dubyak. 2007. Nonclassical IL-1β secretion stimulated by $P2X_7$ receptors is dependent on inflammasome activation and correlated with exosome release in murine macrophages. *J. Immunol.* 179: 1913–1925.
46. Elliott, J. I., A. Sardini, J. C. Cooper, D. R. Alexander, S. Davanture, G. Chimini, and C. F. Higgins. 2006. Phosphatidylserine exposure in B lymphocytes: a role for lipid packing. *Blood* 108: 1611–1617.
47. Adriouch, S., C. Dox, V. Welge, M. Seman, F. Koch-Nolte, and F. Haag. 2002. Cutting edge: a natural P451L mutation in the cytoplasmic domain impairs the function of the mouse $P2X_7$ receptor. *J. Immunol.* 169: 4108–4112.
48. Moreschi, I., S. Bruzzone, R. A. Nicholas, F. Fruscione, L. Sturla, F. Benvenuto, C. Usai, S. Meis, M. U. Kassack, E. Zocchi, and A. De Flora. 2006. Extracellular NAD^+ is an agonist of the human P2Y11 purinergic receptor in human granulocytes. *J. Biol. Chem.* 281: 31419–31429.
49. Nuttle, L. C., and G. R. Dubyak. 1994. Differential activation of cation channels and non-selective pores by macrophage P2z purinergic receptors expressed in *Xenopus* oocytes. *J. Biol. Chem.* 269: 13988–13996.
50. Gudipaty, L., B. D. Humphreys, G. Buell, and G. R. Dubyak. 2001. Regulation of $P2X_7$ nucleotide receptor function in human monocytes by extracellular ions and receptor density. *Am. J. Physiol.* 280: C943–C953.
51. Rozengurt, E., and L. A. Heppel. 1975. A specific effect of external ATP on the permeability of transformed 3T3 cells. *Biochem. Biophys. Res. Commun.* 67: 1581–1588.

52. Rozengurt, E., L. A. Heppel, and I. Friedberg. 1977. Effect of exogenous ATP on the permeability properties of transformed cultures of mouse cell lines. *J. Biol. Chem.* 252: 4584–4590.
53. Rozengurt, E., and L. A. Heppel. 1979. Reciprocal control of membrane permeability of transformed cultures of mouse cell lines by external and internal ATP. *J. Biol. Chem.* 254: 708–714.
54. Labasi, J. M., N. Petrushova, C. Donovan, S. McCurdy, P. Lira, M. M. Payette, W. Brissette, J. R. Wicks, L. Audoly, and C. A. Gabel. 2002. Absence of the P2X$_7$ receptor alters leukocyte function and attenuates an inflammatory response. *J. Immunol.* 168: 6436–6445.
55. Gonnord, P., C. Delarasse, R. Auger, K. Benihoud, M. Prigent, M. H. Cuif, C. Lamaze, and J. M. Kanellopoulos. 2009. Palmitoylation of the P2X$_7$ receptor, an ATP-gated channel, controls its expression and association with lipid rafts. *FASEB J.* 23: 795–805.
56. Takenouchi, T., M. Sato, and H. Kitani. 2007. Lysophosphatidylcholine potentiates Ca2$^+$ influx, pore formation and p44/42 MAP kinase phosphorylation mediated by P2X$_7$ receptor activation in mouse microglial cells. *J. Neurochem.* 102: 1518–1532.
57. Adriouch, S., S. Hubert, S. Pechberty, F. Koch-Nolte, F. Haag, and M. Seman. 2007. NAD$^+$ released during inflammation participates in T cell homeostasis by inducing ART2-mediated death of naive T cells in vivo. *J. Immunol.* 179: 186–194.
58. Krebs, C., S. Adriouch, F. Braasch, W. Koestner, E. H. Leiter, M. Seman, F. E. Lund, N. Oppenheimer, F. Haag, and F. Koch-Nolte. 2005. CD38 controls ADP-ribosyltransferase-2-catalyzed ADP-ribosylation of T cell surface proteins. *J. Immunol.* 174: 3298–3305.
59. Taylor, S. R., M. Gonzalez-Begne, D. K. Sojka, J. C. Richardson, S. A. Sheardown, S. M. Harrison, C. D. Pusey, F. W. Tam, and J. I. Elliott. Lymphocytes from P2X$_7$-deficient mice exhibit enhanced P2X$_7$ responses. *J. Leukocyte Biol.* In press.
60. Vial, C., J. A. Roberts, and R. J. Evans. 2004. Molecular properties of ATP-gated P2X receptor ion channels. *Trends Pharmacol. Sci.* 25: 487–493.
61. Marquez-Klaka, B., J. Rettinger, Y. Bhargava, T. Eisele, and A. Nicke. 2007. Identification of an intersubunit cross-link between substituted cysteine residues located in the putative ATP binding site of the P2X1 receptor. *J. Neurosci.* 27: 1456–1466.
62. Marquez-Klaka, B., J. Rettinger, and A. Nicke. 2009. Inter-subunit disulfide cross-linking in homomeric and heteromeric P2X receptors. *Eur. Biophys. J.* 38: 329–338.
63. Rassendren, F., G. N. Buell, C. Virginio, G. Collo, R. A. North, and A. Surprenant. 1997. The permeabilizing ATP receptor P2X$_7$: cloning and expression of a human cDNA. *J. Biol. Chem.* 272: 5482–5486.
64. Haag, F., F. Koch-Nolte, M. Kuhl, S. Lorenzen, and H. G. Thiele. 1994. Premature stop codons inactivate the RT6 genes of the human and chimpanzee species. *J. Mol. Biol.* 243: 537–546.
65. Donnelly, L. E., N. B. Rendell, S. Murray, J. R. Allport, G. Lo, P. Kefalas, G. W. Taylor, and J. MacDermot. 1996. Arginine-specific mono(ADP-ribosyl)-transferase activity on the surface of human polymorphonuclear neutrophil leucocytes. *Biochem. J.* 315: 635–641.
66. Paone, G., A. Wada, L. A. Stevens, A. Matin, T. Hirayama, R. L. Levine, and J. Moss. 2002. ADP ribosylation of human neutrophil peptide-1 regulates its biological properties. *Proc. Natl. Acad. Sci. USA* 99: 8231–8235.
67. Balducci, E., K. Horiba, J. Usuki, M. Park, V. J. Ferrans, and J. Moss. 1999. Selective expression of RT6 superfamily in human bronchial epithelial cells. *Am. J. Respir. Cell Mol. Biol.* 21: 337–346.
68. Balducci, E., L. G. Micossi, E. Soldaini, and R. Rappuoli. 2007. Expression and selective up-regulation of toxin-related mono ADP-ribosyltransferases by pathogen-associated molecular patterns in alveolar epithelial cells. *FEBS Lett.* 581: 4199–4204.
69. Braren, R., G. Glowacki, M. Nissen, F. Haag, and F. Koch-Nolte. 1998. Molecular characterization and expression of the gene for mouse NAD$^+$:arginine ecto-mono(ADP-ribosyl)transferase, Art1. *Biochem. J.* 336: 561–568.
70. Hong, S., A. Brass, M. Seman, F. Haag, F. Koch-Nolte, and G. R. Dubyak. Basal and inducible expression of the thiol-sensitive ART2.1 ecto-ADP-ribosyltransferase in myeloid and lymphoid leukocytes. *Purinergic Signal.* In press.